

# Sparse signal recovery and source localization via covariance learning

Esa Ollila, *Senior Member, IEEE*

**Abstract**—In the Multiple Measurements Vector (MMV) model, measurement vectors are connected to unknown, jointly sparse signal vectors through a linear regression model employing a single known measurement matrix (or dictionary). Typically, the number of atoms (columns of the dictionary) is greater than the number measurements and the sparse signal recovery problem is generally ill-posed. In this paper, we treat the signals and measurement noise as independent Gaussian random vectors with unknown signal covariance matrix and noise variance, respectively, and derive fixed point (FP) equation for solving the likelihood equation for signal powers, thereby enabling the recovery of the sparse signal support (sources with non-zero variances). Two practical algorithms, a block coordinate descent (BCD) and a cyclic coordinate descent (CCD) algorithms, that leverage on the FP characterization of the likelihood equation are then proposed. Additionally, a greedy pursuit method, analogous to popular simultaneous orthogonal matching pursuit (OMP), is introduced. Our numerical examples demonstrate effectiveness of the proposed covariance learning (CL) algorithms both in classic sparse signal recovery as well as in direction-of-arrival (DOA) estimation problems where they perform favourably compared to the state-of-the-art algorithms under a broad variety of settings.

**Index Terms**—Multiple measurements vector, sparse signal recovery, direction-of-arrival estimation, orthogonal matching pursuit, fixed-point algorithm, sparse Bayesian learning.

## I. INTRODUCTION

IN THE *multiple measurements vector* (MMV) [1] model, the measurement vectors  $\mathbf{y}_l \in \mathbb{C}^N$  follow the generative model

$$\mathbf{y}_l = \mathbf{A}\mathbf{x}_l + \mathbf{e}_l, \quad l = 1, \dots, L, \quad (1)$$

where  $\mathbf{A} = (\mathbf{a}_1 \cdots \mathbf{a}_M) \in \mathbb{C}^{N \times M}$  is a fixed (known) overcomplete matrix ( $M > N$ ) and  $\mathbf{e}_l \in \mathbb{C}^N$  is an unobserved zero mean white noise random vector, i.e.,  $\text{cov}(\mathbf{e}_l) = \sigma^2 \mathbf{I}$ . Matrix  $\mathbf{A}$  is called the *dictionary* or *measurement matrix*, and its column vectors  $\mathbf{a}_i$  are referred to as *atoms*. The unobserved random signal vectors  $\mathbf{x}_l = (x_{l1}, \dots, x_{lM})^\top$ ,  $l = 1, \dots, L$  are assumed to be sparse, i.e., most of their elements are zero.

Letting  $\mathbf{Y} = (\mathbf{y}_1 \cdots \mathbf{y}_L) \in \mathbb{C}^{N \times L}$  to denote the matrix of measurement vectors, we can write the model (1) in matrix form as

$$\mathbf{Y} = \mathbf{A}\mathbf{X} + \mathbf{E}, \quad (2)$$

where matrices  $\mathbf{X} = (x_{ml}) \in \mathbb{C}^{M \times L}$  and  $\mathbf{E} = (e_{nl}) \in \mathbb{C}^{N \times L}$  contain the signal and error vectors as columns, respectively. The key assumption underlying the MMV model is that the signal matrix  $\mathbf{X}$  is  $K$ -row-sparse, i.e., at most  $K$  rows of  $\mathbf{X}$

contain non-zero entries. The rowsupport of  $\mathbf{X} \in \mathbb{C}^{M \times L}$  is the index set of rows containing non-zero elements:

$$\mathcal{M} = \text{supp}(\mathbf{X}) = \{i \in \llbracket M \rrbracket : x_{ij} \neq 0 \text{ for some } j \in \llbracket L \rrbracket\}$$

where  $\llbracket M \rrbracket = \{1, \dots, M\}$ . Since  $\mathbf{X}$  is  $K$ -row-sparse, i.e.,  $|\text{supp}(\mathbf{X})| = K$ , joint estimation can lead both to computational advantages and increased reconstruction accuracy [1]–[6]. In sparse signal recovery (SSR) problems, the object of interest is identifying the support  $\mathcal{M}$ , given only the data  $\mathbf{Y}$ , the dictionary  $\mathbf{A}$ , and the sparsity level  $K$ .

In this paper, the source signal vectors  $\mathbf{x}_l$  are modelled as i.i.d. circular Gaussian random vectors with independent elements and zero mean. Additionally,  $\mathbf{x}_l$ -s are assumed statistically independent of noise  $\mathbf{e}_l$ ,  $l = 1, \dots, L$ . This implies that  $\mathbf{y}_l \sim \mathcal{CN}_N(\mathbf{0}, \Sigma)$ , where the positive definite Hermitian (PDH)  $N \times N$  covariance matrix  $\Sigma = \text{cov}(\mathbf{y}_l)$  has the form

$$\Sigma = \mathbf{A}\mathbf{\Gamma}\mathbf{A}^H + \sigma^2 \mathbf{I} = \sum_{i=1}^M \gamma_i \mathbf{a}_i \mathbf{a}_i^H + \sigma^2 \mathbf{I}. \quad (3)$$

where the signal covariance matrix  $\mathbf{\Gamma} = \text{cov}(\mathbf{x}_l) = \text{diag}(\boldsymbol{\gamma})$  is a diagonal matrix and  $\boldsymbol{\gamma} \in \mathbb{R}_{\geq 0}^M$  is a vector of signal powers with only  $K$  non-zero elements. Hence,  $\mathcal{M} = \text{supp}(\mathbf{X}) = \text{supp}(\boldsymbol{\gamma})$ , and *covariance learning* (CL-)based support recovery algorithms can be constructed by minimizing the negative log-likelihood function (LLF) of the data  $\mathbf{Y}$ , defined by (after scaling by  $1/L$  and ignoring additive constants)

$$\begin{aligned} \ell(\boldsymbol{\gamma}, \sigma^2 \mid \mathbf{Y}, \mathbf{A}) = & \text{tr}((\mathbf{A} \text{diag}(\boldsymbol{\gamma}) \mathbf{A}^H + \sigma^2 \mathbf{I})^{-1} \hat{\Sigma}) \\ & + \log |\mathbf{A} \text{diag}(\boldsymbol{\gamma}) \mathbf{A}^H + \sigma^2 \mathbf{I}| \end{aligned} \quad (4)$$

where  $\hat{\Sigma}$  is the sample covariance matrix (SCM),

$$\hat{\Sigma} = \frac{1}{L} \sum_{l=1}^L \mathbf{y}_l \mathbf{y}_l^H = L^{-1} \mathbf{Y} \mathbf{Y}^H,$$

and  $\text{tr}(\cdot)$  and  $|\cdot|$  denote the matrix trace and determinant.

Approaches for tackling the MMV problem can be categorized into modeling and non-modeling methods. The non-modelling category involves treating  $\mathbf{x}_l$ -s as deterministic latent signal sequences. Then  $\mathbf{X}$  and its rowsupport are determined by either using convex relaxation based optimization methods (e.g.,  $\ell_1$ -minimization) or greedy pursuit algorithms, such as simultaneous orthogonal matching pursuit (SOMP) [2] or the simultaneous normalized iterative hard thresholding (SNIHT) [6]. In the modeling category, the variables  $\mathbf{x}_l$  are considered random, and the widely assumed Gaussianity of both source signals and noise gives rise to stated maximum likelihood (ML) estimation problem. The objective is to determine the minimizer of (4) along with the identification of

Esa Ollila is with the Department of Information and Communications Engineering, Aalto University, FI-00076 Aalto, Finland (e-mail: esa.ollila@aalto.fi).

the support of non-zero source powers. A popular Bayesian approach, sparse Bayesian learning (SBL) [7], regards signal powers ( $\gamma_i$ ) as random hyperparameters governed by a hierarchical prior distribution. An innovative hybrid approach, known as M-SBL algorithm [8], [9], employs an empirical Bayes method to construct an EM algorithm for solving (4). This algorithm proceeds as outlined below, assuming a known value for the noise power ( $\sigma^2$ ):

1) **Initialize:** Set  $\mathbf{\Gamma}^{(0)} = \text{diag}(\gamma^{(0)})$  for some initial  $\gamma^{(0)} \in \mathbb{R}_{\geq 0}^M$ , and  $\mathbf{t} = 0$ .

2) **E-step:**

$$\begin{aligned}\mathbf{\Sigma}^{(\mathbf{t})} &= \mathbf{A}\mathbf{\Gamma}^{(\mathbf{t})}\mathbf{A}^H + \sigma^2\mathbf{I} \\ \mathbf{X}^{(\mathbf{t})} &= \mathbf{\Gamma}^{(\mathbf{t})}\mathbf{A}^H(\mathbf{\Sigma}^{(\mathbf{t})})^{-1}\mathbf{Y}, \\ \mathbf{\Sigma}_x^{(\mathbf{t})} &= \mathbf{\Gamma}^{(\mathbf{t})} - \mathbf{\Gamma}^{(\mathbf{t})}\mathbf{A}^H(\mathbf{\Sigma}^{(\mathbf{t})})^{-1}\mathbf{A}\mathbf{\Gamma}^{(\mathbf{t})}\end{aligned}$$

3) **M-step:**  $\mathbf{\Gamma}^{(\mathbf{t}+1)} = \text{diag}(L^{-1}\mathbf{X}^{(\mathbf{t})}\mathbf{X}^{(\mathbf{t})H} + \mathbf{\Sigma}_x^{(\mathbf{t})})$

4) If not converged, then increment  $\mathbf{t}$  and repeat steps 1-3.

M-SBL method is computationally demanding, and is known to have slow convergence, which often prohibits its uses even when number of atoms  $M$  is only moderately large. Although some faster fixed point SBL update rules have been proposed (e.g., [8, eq. (19)]) these often provide much worse performance than the original slower rule. The CL algorithms proposed in this paper avoid estimation of  $\mathbf{X}$ , distinguishing them from methods such as M-SBL, SOMP, or SNIHT which all require iterative updates of the unknown source signal matrix. Another disadvantage of M-SBL is the assumption that  $\sigma^2$  is known. Although M-step can be modified for joint estimation of  $\sigma^2$ , as mentioned in [7], [10], they tend to provide poor estimation results, which is also attested in our numerical studies. Additionally, the estimate of  $\gamma$  is not necessarily very sparse, but is post-processed by pruning (setting to zero all but  $K$ -largest elements of final iterate  $\hat{\gamma}$ ).

The CL-based iterative FP algorithms proposed in this work share similarity to iterative adaptive approach (IAA) algorithm [11]. IAA solves a weighted LS cost function for source waveforms  $\{x_{ml}\}_{l=1}^L$  and iteratively recalculates the source signal waveforms and their powers. The convergence of IAA was not shown but was supported by the observation that IAA iterates of source powers can be interpreted as approximate solutions to Gaussian LLF [11, Appendix A]. Another closely related technique is Sparse Asymptotic Minimum Variance (SAMV) method [12] that finds the source powers and the variance that minimize the asymptotic minimum variance (AMV) criterion. Third related work is [13] where the source powers are solved via cyclic coordinatewise optimization (CWO) of the LLF in (7). Our CL-based scheme aims at directly solving likelihood equation (i.e.) for signal powers. This is accomplished by characterizing the MLE as solution to a fixed point (FP) equation. This approach enables the formulation of a practical block-coordinate descent (BCD) and cyclic coordinate (CCD) algorithms that leverage the FP characterization. Moreover, it paves the way for the design of a greedy pursuit algorithm that is analogous to SOMP in the classic SSR setting with deterministic source waveforms.

The paper is structured as follows. In Section II, we derive the FP equation to solve the i.e. for signal powers, thus

allowing to recover the signal support (non-zero variances). Two iterative FP algorithms, a BCD- and CCD-based FP algorithms are then proposed. A greedy pursuit method analogous to SOMP is derived in Section III. The effectiveness of the proposed CL-methods in SSR are validated in Section IV via simulation studies. Application to source localization is addressed in Section V. In both problem the proposed CL approaches perform favourably compared to the state-of-the-art algorithms under a broad variety of settings. Finally, Section VI concludes.

*Notations:*  $\mathbf{a}_{\mathcal{M}}$  denotes the components of  $\mathbf{a}$  corresponding to support set  $\mathcal{M}$  with  $|\mathcal{M}| = K$ . For any  $n \times m$  matrix  $\mathbf{A}$  we denote by  $\mathbf{A}_{\mathcal{M}}$  the  $n \times K$  submatrix of  $\mathbf{A}$  restricted to the columns of  $\mathbf{A}$  indexed by set  $\mathcal{M}$ . By  $\mathbf{A}_{\mathcal{M}}$ : we denote the  $K \times m$  submatrix of  $\mathbf{A}$  restricted to the rows of  $\mathbf{A}$  indexed by set  $\mathcal{M}$ . When the boolean parameter `peak` equals `true` (resp. `false`), then the operator  $H_K(\mathbf{a}, \text{peak})$  selectively retains only the  $K$  largest peaks (resp. elements) of the vector  $\mathbf{a}$  and set other elements to zero. Note that  $\text{supp}(H_K(\mathbf{a}, \text{true}))$  will then return the indices of the  $K$  largest elements of vector  $\mathbf{a}$ . We use  $\mathbf{A}^+ = (\mathbf{A}^H\mathbf{A})^{-1}\mathbf{A}^H$  to denote the pseudo-inverse of matrix  $\mathbf{A}$  with full column rank, and  $(\cdot)_+ = \max(\cdot, 0)$  an operator that keeps the positive part of its argument. We use  $\text{diag}(\cdot)$  in two distinct contexts:  $\text{diag}(\mathbf{A})$  denotes an  $N$ -vector comprising the diagonal elements of an  $N \times N$  matrix  $\mathbf{A}$ , whereas  $\text{diag}(\mathbf{a})$  signifies an  $N \times N$  diagonal matrix with its diagonal elements from the  $N$ -vector  $\mathbf{a}$ .

## II. SPARSE ITERATIVE COVARIANCE LEARNING

Our objective in this section is to find a minimizer of (4) under the constraint that  $\gamma$  is  $K$ -sparse. We consider two forms of sparsity:

- **$K$ -sparsity** signifies the search for  $K$ -largest elements of  $\gamma$ .
- **$K$ -peaksparsity** signifies the search for  $K$ -largest peaks of  $\gamma$ .

$K$ -sparsity is the conventional form of sparsity occurring in SSR problems while peaksparsity appears in source localization problems, e.g., spectral line estimation (SLE) [14] of narrowband sources or SSR-based *Direction-of-Arrival (DOA)* estimation [15] in sensor array processing. In the latter case, atoms  $\mathbf{a}_i$  are steering vectors at candidate DOAs chosen from a predefined grid in the angle space. Atoms that reveal high mutual coherence with the steering vector of the true DOA,  $\mathbf{a}(\theta_k)$ , form a cluster with similar signal powers. The extent of coherence depends on the density of the angle grid ( $M$ ), the proximity of these clusters (i.e., closeness of true source DOAs), as well as the sample size ( $L$ ). In the case of SLE, off-grid frequencies resulting from sampling lead to the leakage of energy from component signals into adjacent frequency bins, resulting to sidelobes surrounding the frequency of the sources.

### A. Fixed-point iteration of $\gamma$

Using

$$\frac{\partial \Sigma^{-1}}{\partial \gamma_i} = -\Sigma^{-1} \frac{\partial \Sigma}{\partial \gamma_i} \Sigma^{-1} = -\Sigma^{-1} \mathbf{a}_i \mathbf{a}_i^H \Sigma^{-1}, \quad (5)$$

$$\frac{\partial \log |\Sigma|}{\partial \gamma_i} = \text{tr} \left( \Sigma^{-1} \frac{\partial \Sigma}{\partial \gamma_i} \right) = \mathbf{a}_i^H \Sigma^{-1} \mathbf{a}_i \quad (6)$$

the *likelihood equation (l.e.)* w.r.t. co-ordinate  $\gamma_i$  is obtained by setting the derivative of LLF  $\ell$  in (4) equal to zero

$$0 = \frac{\partial \ell(\gamma, \sigma^2)}{\partial \gamma_i} \Leftrightarrow 0 = -\mathbf{a}_i^H \Sigma^{-1} \hat{\Sigma} \Sigma^{-1} \mathbf{a}_i + \mathbf{a}_i^H \Sigma^{-1} \mathbf{a}_i. \quad (7)$$

Define

$$\Sigma_{\setminus i} = \sum_{j \neq i} \gamma_j \mathbf{a}_j \mathbf{a}_j^H + \sigma^2 \mathbf{I} = \Sigma - \gamma_i \mathbf{a}_i \mathbf{a}_i^H \quad (8)$$

as the covariance matrix of  $\mathbf{y}_1$ -s when the contribution from the  $i^{\text{th}}$  source signal is removed. Next lemma provides FP equation for  $\gamma$  parameter.

**Lemma 1.** *The solution to l.e. in (7) can be expressed as a fixed-point equation:*

$$\gamma = \mathcal{H}(\gamma, \sigma^2)$$

where  $i^{\text{th}}$  coordinate function of  $\mathcal{H}$  is

$$\mathcal{H}_i(\gamma, \sigma^2) = \frac{\mathbf{a}_i^H \Sigma_{\setminus i}^{-1} (\hat{\Sigma} - \Sigma_{\setminus i}) \Sigma_{\setminus i}^{-1} \mathbf{a}_i}{(\mathbf{a}_i^H \Sigma_{\setminus i}^{-1} \mathbf{a}_i)^2} \quad (9)$$

$$= \frac{\mathbf{a}_i^H \Sigma_{\setminus i}^{-1} \hat{\Sigma} \Sigma_{\setminus i}^{-1} \mathbf{a}_i}{(\mathbf{a}_i^H \Sigma_{\setminus i}^{-1} \mathbf{a}_i)^2} - \frac{1}{\mathbf{a}_i^H \Sigma_{\setminus i}^{-1} \mathbf{a}_i} \quad (10)$$

$$= \frac{\mathbf{a}_i^H \Sigma^{-1} \hat{\Sigma} \Sigma^{-1} \mathbf{a}_i}{(\mathbf{a}_i^H \Sigma^{-1} \mathbf{a}_i)^2} - \frac{1}{\mathbf{a}_i^H \Sigma_{\setminus i}^{-1} \mathbf{a}_i}, \quad (11)$$

and where

$$\frac{1}{\mathbf{a}_i^H \Sigma_{\setminus i}^{-1} \mathbf{a}_i} = \frac{1}{\mathbf{a}_i^H \Sigma^{-1} \mathbf{a}_i} - \gamma_i. \quad (12)$$

*Proof.* By Sherman-Morrison formula,

$$(\mathbf{A} + \mathbf{u}\mathbf{v}^H)^{-1} = \mathbf{A}^{-1} - \mathbf{A}^{-1} \mathbf{u}\mathbf{v}^H \mathbf{A}^{-1} / (1 + \mathbf{v}^H \mathbf{A}^{-1} \mathbf{u}) \quad (13)$$

we have that

$$\begin{aligned} \mathbf{a}_i^H \Sigma^{-1} \mathbf{b} &= \mathbf{a}_i^H (\Sigma_{\setminus i} + \gamma_i \mathbf{a}_i \mathbf{a}_i^H)^{-1} \mathbf{b} \\ &= \mathbf{a}_i^H \Sigma_{\setminus i}^{-1} \mathbf{b} - \frac{\mathbf{a}_i^H \Sigma_{\setminus i}^{-1} \mathbf{a}_i \mathbf{a}_i^H \Sigma_{\setminus i}^{-1} \mathbf{b}}{1 + \gamma_i \mathbf{a}_i^H \Sigma_{\setminus i}^{-1} \mathbf{a}_i} \\ &= \mathbf{a}_i^H \Sigma_{\setminus i}^{-1} \mathbf{b} \left( 1 - \frac{\mathbf{a}_i^H \Sigma_{\setminus i}^{-1} \mathbf{a}_i}{1 + \gamma_i \mathbf{a}_i^H \Sigma_{\setminus i}^{-1} \mathbf{a}_i} \right) \\ &= \frac{\mathbf{a}_i^H \Sigma_{\setminus i}^{-1} \mathbf{b}}{1 + \gamma_i \mathbf{a}_i^H \Sigma_{\setminus i}^{-1} \mathbf{a}_i} \end{aligned}$$

for any  $N$ -vector  $\mathbf{b}$ . Applying this formula (twice to the left hand side and once to the right hand side) of the likelihood identity

$$\mathbf{a}_i^H \Sigma^{-1} \hat{\Sigma} \Sigma^{-1} \mathbf{a}_i = \mathbf{a}_i^H \Sigma^{-1} \mathbf{a}_i$$

as expressed by (7), we may write it in the form

$$\mathbf{a}_i^H \Sigma_{\setminus i}^{-1} \hat{\Sigma} \Sigma_{\setminus i}^{-1} \mathbf{a}_i = \mathbf{a}_i^H \Sigma_{\setminus i}^{-1} \mathbf{a}_i (1 + \gamma_i \mathbf{a}_i^H \Sigma_{\setminus i}^{-1} \mathbf{a}_i). \quad (14)$$

Then solving  $\gamma_i$  from (14) yields (10). Also notice that one may express (10) in the form (9) by taking  $(\mathbf{a}_i^H \Sigma_{\setminus i}^{-1} \mathbf{a}_i)^2$  as common denominator for both terms. By Sherman-Morrison formula (13) and relation  $\Sigma_{\setminus i} = \Sigma - \gamma_i \mathbf{a}_i \mathbf{a}_i^H$ , we also have that

$$\mathbf{a}_i^H \Sigma_{\setminus i}^{-1} \mathbf{b} = \frac{\mathbf{a}_i^H \Sigma^{-1} \mathbf{b}}{1 - \gamma_i \mathbf{a}_i^H \Sigma^{-1} \mathbf{a}_i} \quad (15)$$

which again holds for any  $N$ -vector  $\mathbf{b}$ . Applying (15) to (10) yields after some simple algebra the stated equation (11). Next notice that by taking inverses of both sides of (15) yields the identity

$$\frac{1}{\mathbf{a}_i^H \Sigma_{\setminus i}^{-1} \mathbf{b}} = \frac{1}{\mathbf{a}_i^H \Sigma^{-1} \mathbf{b}} - \gamma_i. \quad (16)$$

Then substituting  $\mathbf{b} = \mathbf{a}_i$  in (16) yields the identity (12).  $\square$

Expressions (11) and (12) suggest the following FP update:

$$\begin{aligned} \gamma_i^{(t+1)} &= \mathcal{H}_i(\gamma^{(t)}, \sigma^{2(t)}) \\ &= \frac{\mathbf{a}_i^H \Theta^{(t)} \hat{\Sigma} \Theta^{(t)} \mathbf{a}_i}{(\mathbf{a}_i^H \Theta^{(t)} \mathbf{a}_i)^2} - \left( \frac{1}{\mathbf{a}_i^H \Theta^{(t)} \mathbf{a}_i} - \gamma_i^{(t)} \right)_+ \\ &= \gamma_i^{(t)} + \frac{\mathbf{a}_i^H \Theta^{(t)} \hat{\Sigma} \Theta^{(t)} \mathbf{a}_i}{(\mathbf{a}_i^H \Theta^{(t)} \mathbf{a}_i)^2} - \max \left( \frac{1}{\mathbf{a}_i^H \Theta^{(t)} \mathbf{a}_i}, \gamma_i^{(t)} \right) \end{aligned} \quad (17)$$

for each  $i \in \llbracket M \rrbracket$ , where

$$\Theta^{(t)} = (\mathbf{A} \Gamma^{(t)} \mathbf{A}^H + \sigma^{2(t)} \mathbf{I})^{-1},$$

with  $\Gamma^{(t)} = \text{diag}(\gamma^{(t)})$ , denotes the update of the inverse covariance matrix  $\Theta = \Sigma^{-1}$  at  $t^{\text{th}}$  iteration. Note that  $\mathbf{a}_i^H \Sigma_{\setminus i}^{-1} \mathbf{a}_i \geq 0$  and  $(\cdot)_+$  in (17) guarantees the non-negativity of the latter term.

One can express (17) in the form

$$\gamma_i^{(t+1)} = \begin{cases} \gamma_i^{(t)} + d_i^{(t)} & , \text{ if } \gamma_i^{(t)} < \frac{1}{\mathbf{a}_i^H \Theta^{(t)} \mathbf{a}_i} \\ \frac{\mathbf{a}_i^H \Theta^{(t)} \hat{\Sigma} \Theta^{(t)} \mathbf{a}_i}{(\mathbf{a}_i^H \Theta^{(t)} \mathbf{a}_i)^2} & , \text{ if } \gamma_i^{(t)} \geq \frac{1}{\mathbf{a}_i^H \Theta^{(t)} \mathbf{a}_i} \end{cases} \quad (18)$$

where

$$d_i^{(t)} = \frac{\mathbf{a}_i^H \Theta^{(t)} \hat{\Sigma} \Theta^{(t)} \mathbf{a}_i}{(\mathbf{a}_i^H \Theta^{(t)} \mathbf{a}_i)^2} - \frac{1}{\mathbf{a}_i^H \Theta^{(t)} \mathbf{a}_i}. \quad (19)$$

Hence the FP update (18) effectively makes a decision on either to use a coordinate descent update or a power update. Observe from l.e. (7) that

$$-\nabla_{\gamma_i} \ell(\gamma^{(t)}, \sigma^{2(t)}) = \mathbf{a}_i^H \Theta^{(t)} \hat{\Sigma} \Theta^{(t)} \mathbf{a}_i - \mathbf{a}_i^H \Theta^{(t)} \mathbf{a}_i$$

and thus  $d_i^{(t)}$  in (19) can be written in the form

$$d_i^{(t)} = \mu_t \times -\nabla_{\gamma_i} \ell(\gamma^{(t)}, \sigma^{2(t)})$$

where  $\mu_t = (\mathbf{a}_i^H \Theta^{(t)} \mathbf{a}_i)^{-2}$  can be interpreted as adaptive step size. Thus, if  $\gamma_i^{(t)} < (\mathbf{a}_i^H \Theta^{(t)} \mathbf{a}_i)^{-1}$ , then (18) takes step towards the negative gradient with stepsize  $\mu_t$ .

We can find resemblances between the FP update and at least three distinct methods, each derived from different perspectives. First, the update

$$\gamma_i^{(t+1)} = \gamma_i^{(t)} \left[ \frac{\mathbf{a}_i^H \Theta^{(t)} \hat{\Sigma} \Theta^{(t)} \mathbf{a}_i}{(\mathbf{a}_i^H \Theta^{(t)} \mathbf{a}_i)} \right]^b \quad (20)$$

for  $b = 1$  is used in SAMV2 [12] and derived by minimizing asymptotically minimum variance (AMV) criterion. Furthermore, the SBL-variant in [16], termed SBL1 is based on  $b = 1/2$ . These rules do not necessarily converge to a local minimum of LLF  $\ell$  as they are based on an approximation of the l.e.

Second, the coordinatewise optimization (CWO) of the LLF in (7) is proposed in [13], [17]. To elucidate the concept, let us define a scalar function  $\ell_i(d) = \ell(\gamma + d\mathbf{1}_i, \sigma^2 \mid \mathbf{Y}, \mathbf{A})$ , with  $\ell$  in (4), and  $\mathbf{1}_i$  denotes the  $i^{\text{th}}$  canonical basis vector with a single 1 at its  $i^{\text{th}}$  coordinate and 0s elsewhere. Then it can be shown that [13]:

$$d_i = \arg \min_d \ell_i(d) = \frac{\mathbf{a}_i^H \Theta \hat{\Sigma} \Theta \mathbf{a}_i}{(\mathbf{a}_i^H \Theta \mathbf{a}_i)^2} - \frac{1}{\mathbf{a}_i^H \Theta \mathbf{a}_i}.$$

Since signal powers  $\gamma_i$  are non-negative scalars, the coordinate descent update rule proposed in [13] is

$$\gamma_i \leftarrow \gamma_i + \max(d_i, -\gamma_i), \quad (21)$$

which bears similarity to the FP update in (17).

Third, we note that the signal power update in IAA algorithm, as presented in [11, Table II], can be expressed in the following form:

$$\gamma_i^{(t+1)} = \frac{\mathbf{a}_i^H \Theta^{(t)} \hat{\Sigma} \Theta^{(t)} \mathbf{a}_i}{(\mathbf{a}_i^H \Theta^{(t)} \mathbf{a}_i)^2}, \quad i = 1, \dots, M. \quad (22)$$

Despite originating from a different starting point, namely as the minimizer of a weighted least squares cost function, this update demonstrates the most similarity to our FP rule. When comparing with the FP update rule (18), we anticipate that IAA signal power estimate are likely to converge to the same FP, especially when snapshot size is reasonably large.

### B. Update of the noise power $\sigma^2$

Before addressing the estimation of noise variance  $\sigma^2$ , we remind the reader about the following result which follows from [18].

**Lemma 2.** *Assume  $K < N$ . Then the parameters  $\sigma^2 > 0$  and  $\gamma \in \mathbb{R}_{\geq 0}^K$  that minimize  $\ell(\gamma, \sigma^2 \mid \mathbf{Y}, \mathbf{A})$  in (4) are*

$$\hat{\sigma}^2 = \frac{1}{N-K} \text{tr}((\mathbf{I} - \mathbf{A}\mathbf{A}^+) \hat{\Sigma}) \quad (23)$$

and

$$\hat{\gamma} = \text{diag}(\mathbf{A}^+ (\hat{\Sigma} - \hat{\sigma}^2 \mathbf{I}) \mathbf{A}^+)^{-1} \quad (24)$$

where the latter represents an unconstrained MLE, meaning it aligns with MLE when the non-negativity constraint is met, i.e.,  $\hat{\gamma} \in \mathbb{R}_{\geq 0}^K$ .

**Remark 1.** *In scenarios where  $\hat{\gamma}$  in (24) contains negative elements, one can calculate the constrained solution using [19, Algorithm I]. A more straightforward method involves setting the negative elements of  $\hat{\gamma}$  to zero. While this approach does not precisely yield the MLE, it remains consistent in large samples.*

In our iterative algorithm, an update for  $\sigma^2$  is computed in two steps:

- 1) Identify the support as  $\mathcal{M}^{(t)} = \text{supp}(H_K(\gamma^{(t)}, \text{peak}))$
- 2) Update  $\sigma^2$  as minimizer of  $\ell(\gamma, \sigma^2 \mid \mathbf{Y}, \mathbf{A}_{\mathcal{M}^{(t)}})$ :

$$\hat{\sigma}^{2(t)} = \frac{1}{N - |\mathcal{M}^{(t)}|} \text{tr}((\mathbf{I} - \mathbf{A}_{\mathcal{M}^{(t)}} \mathbf{A}_{\mathcal{M}^{(t)}}^+) \hat{\Sigma}) \quad (25)$$

which follows from Lemma 2.

Some other algorithms use different update rules for noise power. For instance, SAMV2 [12] uses

$$\sigma^{2(t+1)} = \frac{\text{tr}((\Theta^{(t)})^2 \hat{\Sigma})}{\text{tr}((\Theta^{(t)})^2)}.$$

while SBL variants of [20] and [16], [21] use the update (25).

### C. Fixed-point algorithms

Next we propose practical algorithms that leverage the FP characterization of the l.e. derived earlier. The first one, tabulated in algorithm 1 is a block-coordinate descent (BCD) algorithm that updates the parameter  $(\gamma, \sigma^2)$  in blocks. First, in line 2 an update of  $\gamma$  is calculated using FP update (17). This is followed by update of the noise variance  $\sigma^2$  in line 4 using (25) while taking into account either the  $K$ -sparsity or  $K$ -peaksparsity of  $\gamma$  (line 3). Then, if the termination condition (line 5) is not met, one updates the inverse covariance matrix (line 6) and continue iterations until convergence. As the termination condition, we use the relative error

$$\|\gamma^{\text{new}} - \gamma^{\text{old}}\|_{\infty} / \|\gamma^{\text{new}}\|_{\infty} < \epsilon \quad (26)$$

where  $\epsilon$  is a tolerance threshold, e.g.,  $\epsilon = 0.5e^{-4}$ . The algorithm also takes as its input the Boolean variable **peak** which is set as **true** when  $K$ -peaksparsity is assumed and **false** when  $K$ -sparsity is assumed.

---

#### Algorithm 1: CL-BCD algorithm

---

**Input** :  $\mathbf{Y}, \mathbf{A}, K, \text{peak}$

**Initialize:**  $\hat{\Sigma} = L^{-1} \mathbf{Y} \mathbf{Y}^H, \gamma = \mathbf{0}, \Theta = [N / \text{tr}(\hat{\Sigma})] \mathbf{I}$

1 **for**  $t = 1, \dots, I_{\text{max}}$  **do**

2      $\gamma \leftarrow (\gamma_i)_{M \times 1}, \gamma_i \leftarrow \frac{\mathbf{a}_i^H \Theta \hat{\Sigma} \Theta \mathbf{a}_i}{(\mathbf{a}_i^H \Theta \mathbf{a}_i)^2} + \left( \gamma_i - \frac{1}{\mathbf{a}_i^H \Theta \mathbf{a}_i} \right)_+$

3      $\mathcal{M} \leftarrow \text{supp}(H_K(\gamma, \text{peak}))$ .

4      $\sigma^2 \leftarrow \frac{1}{N-K} \text{tr}((\mathbf{I} - \mathbf{A}_{\mathcal{M}} \mathbf{A}_{\mathcal{M}}^+) \hat{\Sigma})$

5     **if** *termination condition is met (see text)* **then**

**break**

6      $\Theta \leftarrow (\mathbf{A} \text{diag}(\gamma) \mathbf{A}^H + \sigma^2 \mathbf{I})^{-1}$

**Output** :  $\mathcal{M}, \gamma, \sigma^2$

---

The other proposed method is a cyclic coordinate descent algorithm (CCD) algorithm displayed in algorithm 2 which updates the parameters  $\gamma_1, \dots, \gamma_M, \sigma^2$  cyclically, i.e., minimizing  $\ell(\gamma_1, \dots, \gamma_M, \sigma^2 \mid \mathbf{Y}, \mathbf{A})$  w.r.t. one coordinate at a time while keeping others fixed at their current iterate values, and repeatedly cycles through each coordinate until convergence. Since each signal power ( $\gamma_i$ ) is updated one at a time via FP update rule, the CCD algorithm requires updating  $\Theta$  after each coordinate update. This can be executed in the following manner. Write  $\delta_i = \gamma_i^{\text{new}} - \gamma_i^{\text{old}}$  for the difference

between the new and old signal powers. Then the update for the covariance matrix is

$$\begin{aligned}\Sigma^{\text{new}} &= \sum_{j \neq i} \gamma_j^{\text{old}} \mathbf{a}_j \mathbf{a}_j^H + \gamma_i^{\text{new}} \mathbf{a}_i \mathbf{a}_i^H \\ &= \sum_{j \neq i} \gamma_j^{\text{old}} \mathbf{a}_j \mathbf{a}_j^H + (\gamma_i^{\text{old}} + \delta_i) \mathbf{a}_i \mathbf{a}_i^H \\ &= \Sigma^{\text{old}} + \delta_i \mathbf{a}_i \mathbf{a}_i^H.\end{aligned}$$

Thus using the Sherman-Morrison formula (13), the update for  $\Theta = \Sigma^{-1}$  is given by

$$\Theta^{\text{new}} = (\Sigma^{\text{old}} + \delta_i \mathbf{a}_i \mathbf{a}_i^H)^{-1} = \Theta^{\text{old}} - \frac{\delta_i \Theta^{\text{old}} \mathbf{a}_i \mathbf{a}_i^H \Theta^{\text{old}}}{1 + \delta_i \mathbf{a}_i^H \Theta^{\text{old}} \mathbf{a}_i}.$$

Note that the algorithm cycles through  $\gamma_i$  one at a time in some fixed (but arbitrary) order. Once all signal power estimates are computed, one computes a new update of the noise power  $\sigma_{\text{new}}^2$  while taking into account either  $K$ -sparsity or  $K$ -peaksparcity and reupdates the inverse covariance matrix. Similarly, let  $g = \sigma_{\text{new}}^2 - \sigma_{\text{old}}^2$  denote the difference between the new and old noise powers. Then the covariance matrix update is  $\Sigma^{\text{new}} = \Sigma^{\text{old}} + g\mathbf{I}$  and hence the update for  $\Theta = \Sigma^{-1}$  can be obtained using the Woodbury matrix identity<sup>1</sup>, leading to

$$\Theta^{\text{new}} = \Theta^{\text{old}} - \Theta^{\text{old}} (\Theta^{\text{old}} + g^{-1}\mathbf{I})^{-1} \Theta^{\text{old}}$$

which is given by line 8 in algorithm 2. As a termination rule, we conclude iterations when (26) is satisfied or when the maximum number of cycles (e.g.,  $I_{\text{cycles}} = 500$ ) has been reached.

---

#### Algorithm 2: CL-CCD algorithm

---

**Input** :  $\mathbf{Y}$ ,  $\mathbf{A}$ ,  $K$ , peak  
**Initialize**:  $\hat{\Sigma} = L^{-1} \mathbf{Y} \mathbf{Y}^H$ ,  $\gamma^{\text{old}} = \mathbf{0}$ ,  
 $\sigma_{\text{old}}^2 = N^{-1} \text{tr}(\hat{\Sigma})$ ,  $\Theta = \sigma_{\text{old}}^{-2} \mathbf{I}$

1 **do**  
2   **for**  $i = 1, \dots, M$  **do**  
3      $\gamma_i^{\text{new}} \leftarrow \frac{\mathbf{a}_i^H \Theta \hat{\Sigma} \Theta \mathbf{a}_i}{(\mathbf{a}_i^H \Theta \mathbf{a}_i)^2} + \left( \gamma_i^{\text{old}} - \frac{1}{\mathbf{a}_i^H \Theta \mathbf{a}_i} \right)_+$   
4      $\delta_i \leftarrow \gamma_i^{\text{new}} - \gamma_i^{\text{old}}$   
5      $\Theta \leftarrow \Theta - \frac{\delta_i \Theta \mathbf{a}_i \mathbf{a}_i^H \Theta}{1 + \delta_i \mathbf{a}_i^H \Theta \mathbf{a}_i}$   
6      $\mathcal{M} \leftarrow \text{supp}(H_K(\gamma, \text{peak}))$   
7      $\sigma_{\text{new}}^2 \leftarrow \frac{1}{N-K} \text{tr}((\mathbf{I} - \mathbf{A}_{\mathcal{M}} \mathbf{A}_{\mathcal{M}}^+) \hat{\Sigma})$   
8      $\Theta \leftarrow \Theta - \Theta (\Theta + (\sigma_{\text{new}}^2 - \sigma_{\text{old}}^2)^{-1} \mathbf{I})^{-1} \Theta$   
9   **while** termination condition not met  
**Output** :  $\mathcal{M}$ ,  $\gamma$ ,  $\sigma^2$

---

#### D. Discussion

Both algorithms are converging to the same fixed point, but CL-CCD is often slower due to its coordinate wise updates, particularly if number of atoms ( $M$ ) is large. However, CL-CCD can be useful in problems where there are memory and power limitations on hardware. Namely, in problems where

<sup>1</sup> $(\mathbf{A} + \mathbf{UCV})^{-1} = \mathbf{A}^{-1} - \mathbf{A}^{-1} \mathbf{U} (\mathbf{C}^{-1} + \mathbf{V} \mathbf{A}^{-1} \mathbf{U})^{-1} \mathbf{V} \mathbf{A}^{-1}$

noise power  $\sigma^2$  is known, we can eliminate steps 6 - 8 in algorithm 2, and thus avoid inverting a possibly large dimensional matrix. This is not possible in CL-BCD. This CL-CCD approach with known  $\sigma^2$  is similar to CWO-strategy that was proposed in [13, Algorithm 1]. The difference is that CL-CCD uses faster FP updates while CWO-method uses coordinatewise optimization which often requires more iterations before convergence.

We foresee opportunities for speeding up the CCD algorithm through strategies like choosing the order of updates (e.g., updating  $\gamma_i$ -s in different order) or updating  $\gamma_i$ -s in several blocks instead of coordinatewise. We leave these possibilities as subjects for future research. Additionally, a small threshold can be defined so that when any  $\gamma_i$  becomes sufficiently small (e.g.,  $10^{-12}$ ), the corresponding atom  $\mathbf{a}_i$  is pruned from the model. This can be useful when  $M$  is excessively large. Such a technique can be applied to both BCD and CCD methods.

Finally, we would like to point out some benefits of the proposed FP algorithms. First,  $L > N$  is not required, but the algorithms can be applied even in a single snapshot ( $L = 1$ ) situation. Furthermore, the methods do not require an initial estimates of signal power vector  $\gamma$ . This is in contrast to many other CL methods proposed in the literature such as SPICE [22], M-SBL [8], [9], SBL [21], RVM [9] or SAMV [12].

### III. GREEDY PURSUIT COVARIANCE LEARNING

We first recall the following result from [11].

**Lemma 3.** Consider the conditional likelihood of (4) where source powers  $\gamma_j$  for  $j \neq i$  and the noise variance  $\sigma^2$  are known. Then the conditional negative log-likelihood function for the unknown  $i^{\text{th}}$  source, defined as

$$\begin{aligned}l_i(\gamma \mid \mathbf{Y}, \mathbf{A}, \{\gamma_j\}_{j \neq i}, \sigma^2) \\ = \text{tr}((\Sigma_{\setminus i} + \gamma \mathbf{a}_i \mathbf{a}_i^H)^{-1} \hat{\Sigma}) + \log |\Sigma_{\setminus i} + \gamma \mathbf{a}_i \mathbf{a}_i^H|,\end{aligned}\quad (27)$$

has a unique optimal value

$$\gamma_i = \max \left( \frac{\mathbf{a}_i^H \Sigma_{\setminus i}^{-1} (\hat{\Sigma} - \Sigma_{\setminus i}) \Sigma_{\setminus i}^{-1} \mathbf{a}_i}{(\mathbf{a}_i^H \Sigma_{\setminus i}^{-1} \mathbf{a}_i)^2}, 0 \right), \quad (28)$$

where  $\Sigma_{\setminus i}$  is defined in (8).

*Proof.* The proof of (30) is given in [11, Appendix B].  $\square$

Lemma 3 will serve as the foundation for developing the CL-based Orthogonal Matching Pursuit (CL-OMP) algorithm, presented in algorithm 3. This algorithm follows a matching pursuit strategy similar to the one outlined in [23, Table 3.1].

**Initialization** phase. Set  $k = 0$ , and  $\gamma^{(0)} = \mathbf{0}_{M \times 1}$ ,  $\sigma^{2(0)} = [\text{tr}(\hat{\Sigma})/N] \mathbf{I}$ , and  $\mathcal{M}^{(0)} = \text{supp}(\gamma^{(0)}) = \emptyset$  as initial solutions of signal and noise powers and the signal support, respectively. Then  $\Sigma^{(0)} = \mathbf{A} \text{diag}(\gamma^{(0)}) \mathbf{A}^H + \sigma^{2(0)} \mathbf{I} = \sigma^{2(0)} \mathbf{I}$  is the initial covariance matrix at the start of iterations.

**Main Iteration** phase consists of the following steps:

1) *Sweep*: Compute the errors

$$\epsilon_i = \min_{\gamma \geq 0} l_i(\gamma \mid \mathbf{Y}, \mathbf{A}, \{\gamma_j^{(k)}\}_{j \neq i}, \sigma^{2(k)}) \quad (29)$$



for each  $i \in \llbracket M \rrbracket \setminus \mathcal{M}^{(k)}$  using its unique optimal value as given by Lemma 3:

$$\gamma_i = \max \left( \frac{\mathbf{a}_i^H (\boldsymbol{\Sigma}^{(k)})^{-1} (\hat{\boldsymbol{\Sigma}} - \boldsymbol{\Sigma}^{(k)}) (\boldsymbol{\Sigma}^{(k)})^{-1} \mathbf{a}_i}{(\mathbf{a}_i^H (\boldsymbol{\Sigma}^{(k)})^{-1} \mathbf{a}_i)^2}, 0 \right). \quad (30)$$

The sweep stage is comprised of lines 2 and 3 in algorithm 3.

2) *Update support*: Find a minimizer,  $i_k$  of  $\epsilon_i$ :  $\forall i \notin \mathcal{M}^{(k)}$ ,  $\epsilon_{i_k} \leq \epsilon_i$ , and update the support  $\mathcal{M}^{(k+1)} = \mathcal{M}^{(k)} \cup \{i_k\}$ . This step corresponds to line 4 in algorithm 3.

3) *Update provisional solution*: compute

$$(\hat{\mathbf{g}}, \hat{\sigma}^2) = \arg \min_{\mathbf{g}, \sigma^2} \ell(\mathbf{g}, \sigma^2 \mid \mathbf{Y}, \mathbf{A}_{\mathcal{M}^{(k+1)}}),$$

where  $\ell$  is the LLF defined in (4). These solutions are obtained from Lemma 2 and calculated in lines 5 – 7 in algorithm 3, respectively. The obtained signal power is constrained to be non-negative, which is not exactly the MLE. Alternative option is to compute the true MLE (the constrained solution) using [19, Algorithm 1] as noted in Remark 1.

4) *Update the covariance matrix*: Compute  $\boldsymbol{\Sigma}^{(k+1)} = \mathbf{A}_{\mathcal{M}} \text{diag}(\hat{\mathbf{g}}) \mathbf{A}_{\mathcal{M}}^H + \hat{\sigma}^2 \mathbf{I}$ . This stage is implemented by line 8 in algorithm 3.

5) *Stopping rule*: stop after  $K$  iterations, and otherwise increment  $k$  by 1 and repeat steps 1)-4). It is worth noting that alternative stopping criteria can be employed, such as halting the process when the variance  $\sigma^{2(k)}$  falls below a predefined threshold. This criterion is particularly valuable in applications where the noise level can be accurately estimated or is known a priori.

Note that the sweep stage gives (after some simple algebra) the following value for the error in (29):

$$\epsilon_i = c + \log(1 + \gamma_i \mathbf{a}_i^H \boldsymbol{\Sigma}^{-1} \mathbf{a}_i) - \gamma_i \frac{\mathbf{a}_i^H \boldsymbol{\Sigma}^{-1} \hat{\boldsymbol{\Sigma}} \boldsymbol{\Sigma}^{-1} \mathbf{a}_i}{1 + \gamma_i \mathbf{a}_i^H \boldsymbol{\Sigma}^{-1} \mathbf{a}_i} \quad (31)$$

where we have for simplicity of notation written  $\boldsymbol{\Sigma} = \boldsymbol{\Sigma}^{(k)}$  and where  $c$  denotes an irrelevant constant that is not dependent on  $\gamma_i$ . Thus w.l.o.g. we set  $c = 0$ . Then using that  $\gamma_i$  is given by (30) we can write

$$\begin{aligned} 1 + \gamma_i \mathbf{a}_i^H \boldsymbol{\Sigma}^{-1} \mathbf{a}_i &= 1 + \frac{\mathbf{a}_i^H \boldsymbol{\Sigma}^{-1} (\hat{\boldsymbol{\Sigma}} - \boldsymbol{\Sigma}) \boldsymbol{\Sigma}^{-1} \mathbf{a}_i}{(\mathbf{a}_i^H \boldsymbol{\Sigma}^{-1} \mathbf{a}_i)^2} \mathbf{a}_i^H \boldsymbol{\Sigma}^{-1} \mathbf{a}_i \\ &= 1 + \frac{\mathbf{a}_i^H \boldsymbol{\Sigma}^{-1} \hat{\boldsymbol{\Sigma}} \boldsymbol{\Sigma}^{-1} \mathbf{a}_i - \mathbf{a}_i^H \boldsymbol{\Sigma}^{-1} \mathbf{a}_i}{\mathbf{a}_i^H \boldsymbol{\Sigma}^{-1} \mathbf{a}_i} \\ &= \frac{\mathbf{a}_i^H \boldsymbol{\Sigma}^{-1} \hat{\boldsymbol{\Sigma}} \boldsymbol{\Sigma}^{-1} \mathbf{a}_i}{\mathbf{a}_i^H \boldsymbol{\Sigma}^{-1} \mathbf{a}_i} \end{aligned}$$

in the case that  $\gamma_i > 0$ . Substituting this into the denominator of the last term in (31), we obtain

$$\epsilon_i = \log(1 + \gamma_i \mathbf{a}_i^H \boldsymbol{\Sigma}^{-1} \mathbf{a}_i) - \gamma_i \mathbf{a}_i^H \boldsymbol{\Sigma}^{-1} \mathbf{a}_i. \quad (32)$$

If  $\gamma_i = 0$ , then  $\epsilon_i = 0$ . This explains line 3 in algorithm 3.

In the provisional solution update, one finds the minimizer of  $\ell(\boldsymbol{\gamma}, \sigma^2 \mid \mathbf{Y}, \mathbf{A}_{\mathcal{M}})$  where for notational simplicity we wrote  $\mathcal{M} = \mathcal{M}^{(k+1)}$  for the current support with  $|\mathcal{M}| = k$ . Thus the problem to be solved is

$$\begin{aligned} &\underset{\boldsymbol{\gamma} \in \mathbb{R}_{\geq 0}^k, \sigma^2 > 0}{\text{minimize}} \quad \text{tr}((\mathbf{A}_{\mathcal{M}} \text{diag}(\boldsymbol{\gamma}) \mathbf{A}_{\mathcal{M}}^H + \sigma^2 \mathbf{I})^{-1} \hat{\boldsymbol{\Sigma}}) \\ &\quad + \log |\mathbf{A}_{\mathcal{M}} \text{diag}(\boldsymbol{\gamma}) \mathbf{A}_{\mathcal{M}}^H + \sigma^2 \mathbf{I}|. \end{aligned}$$

As already noted, taking the derivative of this equation w.r.t.  $\gamma_i$  and setting it to zero, gives the i.e.:

$$0 = \mathbf{a}_i^H \boldsymbol{\Sigma}^{-1} (\hat{\boldsymbol{\Sigma}} - \boldsymbol{\Sigma}) \boldsymbol{\Sigma}^{-1} \mathbf{a}_i \quad \forall i \in \mathcal{M}.$$

This in turn implies that in the next iteration  $\gamma_i$  in (30) will take value  $\gamma_i \approx 0$  for  $i \in \mathcal{M}$ . Thus unlikely these columns will be chosen again for the support in the next iterations. This explains the name of this greedy pursuit algorithm: the method is similar to conventional OMP [24] or SOMP [2] where no atom is ever chosen twice in the sweep stage.

---

### Algorithm 3: CL-OMP algorithm

---

**Input** :  $\mathbf{Y}, \mathbf{A}, K$

**Initialize**:  $\hat{\boldsymbol{\Sigma}} = L^{-1} \mathbf{Y} \mathbf{Y}^H, \boldsymbol{\Sigma} = [\text{tr}(\hat{\boldsymbol{\Sigma}})/p] \mathbf{I}, \mathcal{M} = \emptyset$

```

1 for  $k = 1, \dots, M$  do
2    $\boldsymbol{\gamma} = (\gamma_i)_{M \times 1}, \gamma_i \leftarrow \max \left( \frac{\mathbf{a}_i^H \boldsymbol{\Sigma}^{-1} (\hat{\boldsymbol{\Sigma}} - \boldsymbol{\Sigma}) \boldsymbol{\Sigma}^{-1} \mathbf{a}_i}{(\mathbf{a}_i^H \boldsymbol{\Sigma}^{-1} \mathbf{a}_i)^2}, 0 \right)$ 
3    $\boldsymbol{\epsilon} = (\epsilon_i) \leftarrow (\log(1 + \gamma_i \mathbf{a}_i^H \boldsymbol{\Sigma}^{-1} \mathbf{a}_i) - \gamma_i \mathbf{a}_i^H \boldsymbol{\Sigma}^{-1} \mathbf{a}_i)_{M \times 1}$ 
4    $\mathcal{M} \leftarrow \mathcal{M} \cup \{i_k\}$  with  $i_k \leftarrow \arg \min_{i \notin \mathcal{M}} \epsilon_i$ 
5    $\sigma^2 \leftarrow \frac{1}{N-k} \text{tr}((\mathbf{I} - \mathbf{A}_{\mathcal{M}} \mathbf{A}_{\mathcal{M}}^+) \hat{\boldsymbol{\Sigma}})$ 
6    $\boldsymbol{\gamma}_{\mathcal{M}} \leftarrow \max(\text{diag}(\mathbf{A}_{\mathcal{M}}^+ (\hat{\boldsymbol{\Sigma}} - \sigma^2 \mathbf{I}) \mathbf{A}_{\mathcal{M}}^+), 0)$ 
7    $\boldsymbol{\gamma}_{\mathcal{M}^c} \leftarrow \mathbf{0}$ 
8    $\boldsymbol{\Sigma} \leftarrow \mathbf{A} \text{diag}(\boldsymbol{\gamma}) \mathbf{A}^H + \sigma^2 \mathbf{I}$ 
9   if stopping rule is met (see text) then
      $\lfloor$  break

```

**Output** :  $\mathcal{M}, \boldsymbol{\gamma}, \sigma^2$

---

## IV. SPARSE SIGNAL RECOVERY: SIMULATION STUDIES

Next we compare the sparse signal recovery performance of CL-BCD, CL-CCD and CL-OMP to traditional greedy sparse signal recovery algorithms, the **SOMP** [2, Algorithm 3.1] and the **SNIHT** [6, Algorithm 1]. The boolean variable **peak** is thus set to **false** as we assume  $K$ -sparsity in this example. Both SOMP and SNIHT algorithms are designed for MMV model, and return an estimated support  $\mathcal{M}$  of  $K$ -rowsparse signal matrix given the measurement matrix  $\mathbf{Y}$ , the dictionary  $\mathbf{A}$ , and the desired rowsparsity level  $K$ . Finally, since CL-CCD converges to same fixed-point as CL-BCD, the legends display only CL-BCD. Comparison to M-SBL is challenging as it assumes that  $\sigma^2$  is known. However, update rules for  $\sigma^2$  can be integrated into the EM algorithm by replacing the M-step with a joint maximization over  $\sigma^2$  and  $\boldsymbol{\gamma}$ , resulting in the addition of the  $\sigma^2$  update [8, Eq. (21)] to the M-step:

$$\sigma^{2(t+1)} = \frac{\frac{1}{L} \|\mathbf{Y} - \mathbf{A} \mathbf{X}^{(t)}\|_{\text{Fr}}^2}{N - M + \sum_{i=1}^M (\boldsymbol{\Sigma}_x^{(t)})_{ii} / \gamma_i^{(t+1)}}$$

In [8], it was noted that joint estimation can result in severely biased estimates of  $\sigma^2$ , thereby affecting the accuracy of  $\boldsymbol{\gamma}$  estimate. Consequently, the authors in [8] recommend using alternatives such as grid search or other heuristics to estimate  $\sigma^2$ . We report values of M-SBL that utilize the true  $\sigma^2$ , denoted as **M-SBL- $\sigma^2$** , while the version that jointly estimates both  $\sigma^2$  and  $\boldsymbol{\gamma}$  is termed **M-SBL**. We also compare with CWO method

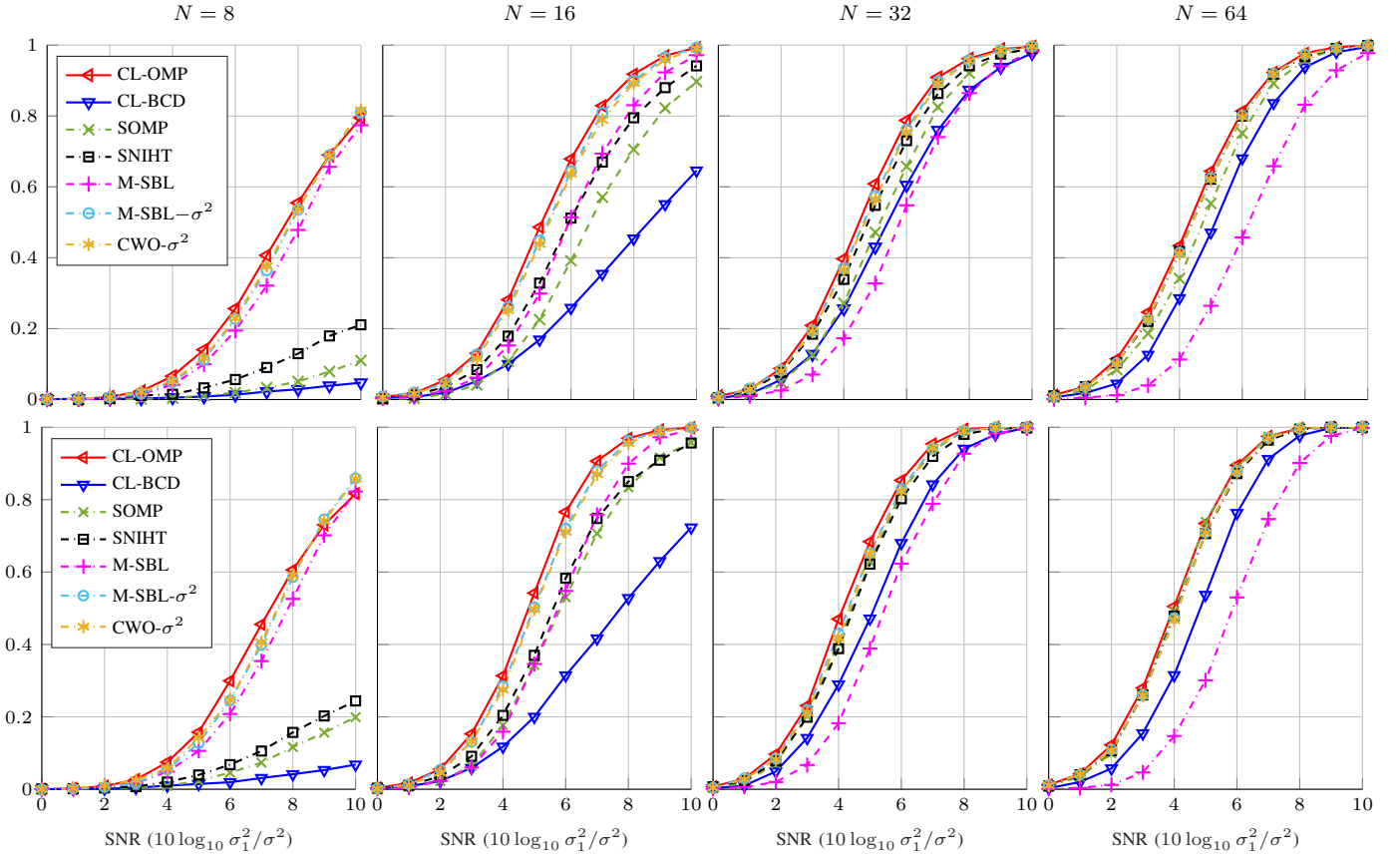


Fig. 1: Comparison of PER rates of different sparse recovery algorithms under a variety of SNR levels when the sources are Gaussian (top panel) and non-Gaussian (bottom panel) and the number of measurements increases from  $N = 8$  to  $N = 64$ ;  $K = 4$ ,  $M = 256$ ,  $L = 16$  and dictionary is a Gaussian measurement matrix.

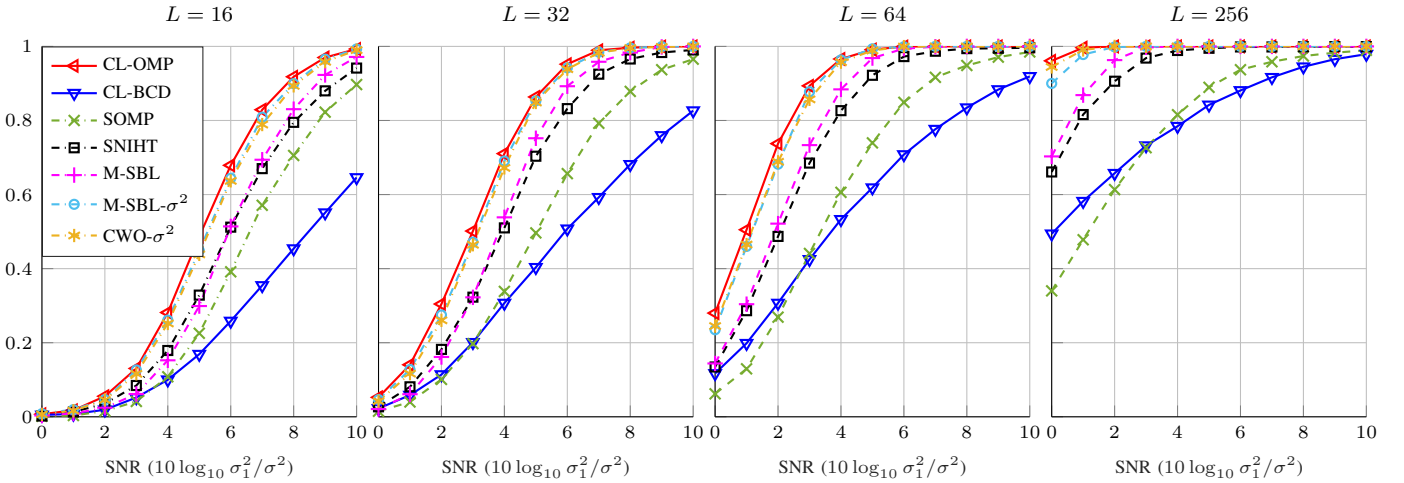


Fig. 2: Comparison of PER rates of different sparse recovery algorithms under a variety of SNR levels when the sources are Gaussian and the number of snapshots increases from  $L = 16$  to  $L = 256$ ;  $N = 16$ ,  $K = 4$ ,  $M = 256$ , and the dictionary is a Gaussian measurement matrix.

of [13, Algorithm 1] which uses signal power updates in (21), and which we term **CWO- $\sigma^2$** , where again the suffix  $\sigma^2$  is used to indicate that this method uses true  $\sigma^2$ . Naturally, M-SBL- $\sigma^2$  and CWO- $\sigma^2$  are not realisable as  $\sigma^2$  is unknown and their performance is only shown as benchmark for best

possible performance.

In our simulations, the matrix  $\mathbf{A}$  is a Gaussian random measurement matrix, i.e., the elements of  $\mathbf{A}$  are drawn from  $\mathcal{CN}(0, 1)$  distribution and the columns are unit-norm normalised as is common in compressed sensing. To form

the  $K$ -row-sparse source signal matrix  $\mathbf{X} \in \mathbb{C}^{M \times L}$ , support  $\mathcal{M} = \text{supp}(\mathbf{X})$  is randomly chosen from  $\{1, \dots, M\}$  without replacement for each Monte-Carlo (MC-)trial. The noise  $\mathbf{E} \in \mathbb{C}^{N \times L}$  have elements that are i.i.d. circular complex Gaussian with unit variance (i.e.,  $\sigma^2 = 1$ ).

As performance measure we use the empirical *probability of exact recovery*,  $\text{PER} = \frac{1}{T} \sum_{t=1}^T \mathbb{I}(\hat{\mathcal{M}}^{(t)} = \mathcal{M}^{(t)})$ , where  $\mathbb{I}(\cdot)$  denotes the indicator function, and  $\hat{\mathcal{M}}^{(t)}$  denotes the estimate of the true signal support  $\mathcal{M}^{(t)}$  for  $t^{\text{th}}$  MC trial. The number of MC trials is  $T = 2000$ , the number of atoms is  $M = 256$ , and the sparsity level is  $K = 4$ . The dimensionality of the measurements  $N$  or the number of measurement vectors  $L$  may vary. Let  $\mathcal{M} = \{i_1, \dots, i_K\}$  be the true support set where  $K = 4$ , and let  $\sigma_1^2 = \gamma_{i_1}$  denote the power of the 1<sup>st</sup> Gaussian source signal. Define the SNR of the first non-zero source sequence as  $10 \log_{10} \sigma_1^2 / \sigma^2$ . For the second, third, and fourth Gaussian sources, we set their SNR levels to be 1 dB, 2 dB, and 4 dB lower than that of the first source, respectively.

The upper panel of Figure 1 displays the PER rates when the number of measurement vectors is fixed ( $L = 16$ ) while the dimensionality of measurements  $N$  grows ( $N = 8, 16, 32$  to  $N = 64$ ). As can be noted, CL-OMP has the best performance for all  $N$  and SNR levels. For example, at SNR = 5dB and  $N = 32$ , the PER rates are 60.1%, 43.0%, 47.2%, 54.8% and 32.8%, 57.45% and 56.55% for the CL-OMP, CL-BCD, SOMP, SNIHT, M-SBL, M-SBL- $\sigma^2$  and CWO- $\sigma^2$ , respectively. Note that M-SBL (which estimates  $\sigma^2$  in M-step) has 25% drop in accuracy compared with M-SBL- $\sigma^2$  (that uses true  $\sigma^2$ ) illustrating the instability of estimating  $\gamma$  and  $\sigma^2$  jointly in the EM algorithm. It can also be noted that the performance of M-SBL deteriorates with the growth of  $N$ . When comparing SNIHT and SOMP, it is observed that SNIHT outperforms SOMP, yet SOMP gradually improves, approaching the performance level of SNIHT as the number of measurements  $N$  increases. While CL-BCD is not performing that well with small  $N$ , it also shows significant improvement as  $N$  increases. When comparing M-SBL- $\sigma^2$  and CWO- $\sigma^2$  we notice that M-SBL- $\sigma^2$  often has slight advantage over CWO- $\sigma^2$  but this comes with extra computational burden.

Next, we explore the impact of the Gaussianity of source signals on method performances. The signals sequences  $x_{il}$  possess a fixed amplitude  $\gamma_i = |x_{il}|^2 > 0$  for all  $l = 1, \dots, L$ , where  $\gamma_i > 0$  for  $i \in \mathcal{M}$  and  $\gamma_i = 0$  otherwise. The phase is a random variable with a uniform distribution,  $\text{Arg}(x_{il}) \sim \text{Unif}(0, 2\pi)$ . In other words,  $\{x_{il}\}$  for  $i \in \mathcal{M}$  forms an i.i.d sample of length  $L$  from a uniform distribution on the complex circle of fixed radius  $\gamma_i$ . The bottom panel of Figure 1 depicts the performance in this scenario. A comparison between the upper and bottom panel figures reveals that the performance of all methods remain consistent even with non-Gaussian sources. Consequently, the performance of CL-methods, designed under the assumption of Gaussianity of source sequences, remains unaffected by the violation of this assumption.

In the next study, dimensionality  $N$  is fixed ( $N = 16$ ), while the number of measurements vectors  $L$  varies. Otherwise the setting is as earlier. Again we note from Figure 2 that CL-OMP uniformly outperforms the other methods for all SNR

levels and snapshot sizes. Consider, for instance, the scenario with  $L = 256$  and a very low SNR of 1 dB. In this case, CL-OMP stands out as the only method achieving a perfect 100% PER rate. Meanwhile, SNIHT and SOMP exhibit PER rates of 81.6% and 47.8%, respectively. The PER rates for M-SBL, M-SBL- $\sigma^2$  and CWO- $\sigma^2$  are 86.8%, 97.8%, 99.0%, respectively. CL-BCD, on the other hand, yields a PER rate of 58.2%, making it notably inferior to its greedy counterpart, CL-OMP. Overall (for all values of  $L$ ) CL-OMP is distinctively more robust to low SNR than conventional greedy methods, SOMP and SNIHT. CL-OMP is also consistently better than M-SBL- $\sigma^2$  and CWO- $\sigma^2$  which are the only methods that have oracle knowledge of the noise power  $\sigma^2$ . We repeated the simulation for non-Gaussian sources scenario, but the results were similar as for Gaussian sources case, and are omitted.

## V. SOURCE LOCALIZATION USING COVARIANCE LEARNING

We consider an array signal model where  $K$  narrowband and farfield source signals imping on an array of  $N$  sensors from distinct DOAs  $\theta_k$ ,  $k = 1, \dots, K$  ( $N > K$ ). The array measurement vectors  $\mathbf{y}_1, \dots, \mathbf{y}_L$ , called *snapshots*, are then modelled as [25], [26]:

$$\mathbf{y}_l = \mathbf{A}(\boldsymbol{\theta})\mathbf{s}_l + \mathbf{e}_l, \quad l = 1, \dots, L \quad (33)$$

where  $\mathbf{s}_l \in \mathbb{C}^K$  is the unobserved zero mean source signal waveforms,  $\mathbf{e}_l \in \mathbb{C}^N$  is the zero mean white noise vector with covariance matrix  $\text{cov}(\mathbf{e}_l) = \sigma^2 \mathbf{I}$ , and  $\mathbf{A}(\boldsymbol{\theta}) = (\mathbf{a}(\theta_1) \dots \mathbf{a}(\theta_K)) \in \mathbb{C}^{N \times K}$  is the array steering matrix. The parameter space of  $\theta_k$  and form of steering vector  $\mathbf{a}(\cdot)$  depend on the array geometry: for example,  $\theta_k \in \mathbb{T} = [-\pi/2, \pi/2]$  and  $(\mathbf{A}(\boldsymbol{\theta}))_{nk} = e^{-j(n-1)\frac{2\pi d}{\lambda} \sin \theta_k}$  for Uniform Linear Array (ULA), where  $\lambda$  is the wavelength and  $d$  is the element spacing between the sensors. The main objective of source localization is to estimate the DOA-s of the sources as accurately as possible.

When both the source signals and the noise are independent complex circular Gaussian random vectors, then the *array covariance matrix*  $\boldsymbol{\Sigma} = \text{cov}(\mathbf{y}_i)$  becomes

$$\boldsymbol{\Sigma} = \mathbf{A}(\boldsymbol{\theta})\boldsymbol{\Sigma}_s\mathbf{A}(\boldsymbol{\theta})^H + \sigma^2\mathbf{I}, \quad (34)$$

where  $\boldsymbol{\Sigma}_s = \text{cov}(\mathbf{s}_i) \in \mathbb{C}^{K \times K}$  is the positive semidefinite signal covariance matrix. If sources signals are statistically independent, then  $\boldsymbol{\Sigma}_s = \text{diag}(\boldsymbol{\sigma}_s^2) = \text{diag}(\sigma_{s,1}^2, \dots, \sigma_{s,K}^2)$ , where  $\sigma_{s,k}^2 > 0$  is the power of the  $k^{\text{th}}$  source. The parameter estimates are found by minimizing the negative LLF:

$$\begin{aligned} \ell(\boldsymbol{\theta}, \boldsymbol{\Sigma}_s, \sigma^2) &= \text{tr}(\boldsymbol{\Sigma}^{-1}\hat{\boldsymbol{\Sigma}}) + \log |\boldsymbol{\Sigma}| \\ &\text{subject to } \boldsymbol{\Sigma} = \mathbf{A}(\boldsymbol{\theta})\boldsymbol{\Sigma}_s\mathbf{A}(\boldsymbol{\theta})^H + \sigma^2\mathbf{I}, \boldsymbol{\Sigma}_s \succeq 0, \sigma^2 > 0 \end{aligned} \quad (35)$$

and called as stochastic maximum likelihood (SML) [25] or unconditional ML (UML) estimators [26]. MLE-s of DOAs are found by solving the concentrated LLF [18], [25], [27]

$$\hat{\boldsymbol{\theta}}_{\text{ML}} = \arg \min_{\boldsymbol{\theta}} \left\{ V(\boldsymbol{\theta}) = \log |\mathbf{A}(\boldsymbol{\theta})\hat{\boldsymbol{\Sigma}}_s\mathbf{A}(\boldsymbol{\theta})^H + \hat{\sigma}^2\mathbf{I}| \right\} \quad (36)$$

where  $\hat{\boldsymbol{\Sigma}}_s = \hat{\boldsymbol{\Sigma}}_s(\boldsymbol{\theta}) = \mathbf{A}^+(\hat{\boldsymbol{\Sigma}} - \hat{\sigma}^2\mathbf{I})\mathbf{A}^H$  and  $\hat{\sigma}^2 = \hat{\sigma}^2(\boldsymbol{\theta})$ , defined in (23), are functions of  $\boldsymbol{\theta}$  via the steering matrix  $\mathbf{A} = \mathbf{A}(\boldsymbol{\theta})$ . Strictly speaking, solving (36) gives MLE-s only when  $\hat{\boldsymbol{\Gamma}}$  is positive semidefinite as was noted in



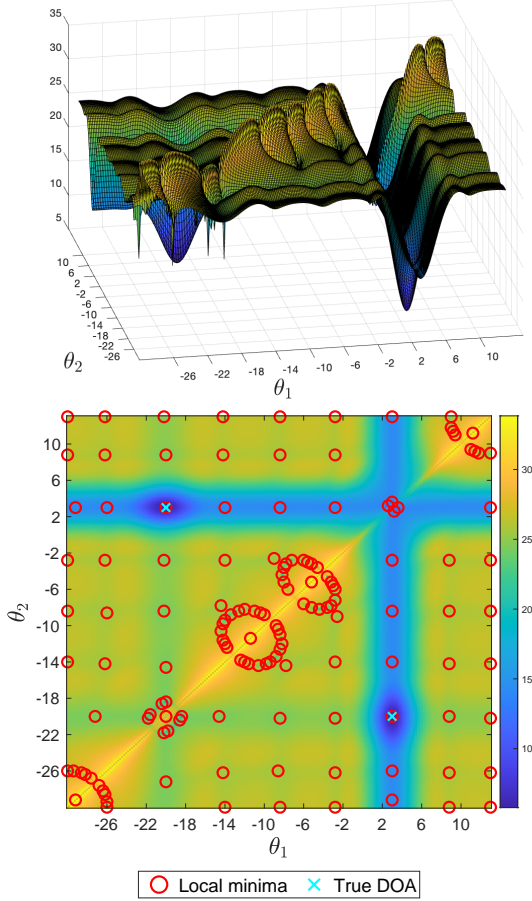


Fig. 3: Criterion  $V(\boldsymbol{\theta}) = V(\theta_1, \theta_2)$  for 2 uncorrelated sources case. The first source at  $\theta_1 = -20^\circ$  has SNR 0 dB and the 2nd source at  $\theta_2 = 3^\circ$  has SNR 3 dB. The array is ULA with half a wavelength interelement spacing.

[19]. Unfortunately, the cost function  $V(\boldsymbol{\theta})$  is highly non-linear function of DOAs, containing dozens of local minimas, thus causing standard approaches like the Newton-Raphson schemes [25]–[27] to fail<sup>2</sup>. To illustrate this claim, we present the cost function  $V(\boldsymbol{\theta})$  in Figure 3 under the conditions where the first source at  $\theta_1 = -20$  has a SNR of 0 dB, while the second source at  $\theta_2 = 3^\circ$  has an SNR of 3 dB. The sources are uncorrelated, and the snapshot size is  $L = 100$ . The array is ULA with half a wavelength interelement spacing. Solving the MLE of DOAs from (36) is thus challenging, but as is demonstrated in our simulation studies, the CL-based DOA algorithms offer a viable alternative, providing accurate approximations of the MLE.

#### A. Source localization via Covariance Learning

We discretize the DOA space (assume  $[-\pi/2, \pi/2)$ ) into  $M$  equidistant grid points  $-\pi/2 \leq \theta'_1 < \dots < \theta'_M < \pi/2$ , where the grid spacing  $\Delta\theta = \theta'_2 - \theta'_1$  determines the angular resolution. Often  $M \gg N$ , where  $M$  can be of several

<sup>2</sup>NR-algorithm will converge to one of the multiple poor local minima unless an highly accurate initial estimate can be given.

thousands to achieve high-resolution DOA estimates. Let  $\mathbf{A} = (\mathbf{a}_1 \dots \mathbf{a}_p) \in \mathbb{C}^{N \times M}$  be the dictionary of the array response vectors  $\mathbf{a}_i = \mathbf{a}(\theta'_i)$ . The groundbreaking work by [15] leveraged the property that if the grid points incorporate the true DOAs, then the array model (33) can be expressed as an MMV model (2) with an exactly  $K$ -rowsparse signal matrix, where  $\mathbf{X}_{\mathcal{M}} = \mathbf{S}$  and  $\mathcal{M}$  denotes the set of indices of the DOAs on the grid. Therefore, DOA estimation is equivalent to solving SSR in the MMV model under a  $K$ -sparsity constraint. Numerous methods approach source localization from this perspective, including works such as [15], [28]–[30]. The MMV formulation naturally lends itself to the use of the CL scheme as well since  $\mathcal{M} = \text{supp}(\boldsymbol{\gamma})$ . Therefore, source localization is equivalent to solving (4) subject to  $|\mathcal{M}| = K$ . CL methods for source localization have been developed for example in [8], [9], [11], [12], [21], [22], [31].

It is important to realise that even if the true DOAs are on-grid, the source power estimates  $\hat{\boldsymbol{\gamma}}$  does not exhibit  $K$ -sparsity but  $K$ -peaksparsity. Namely, the power from  $i^{\text{th}}$  source is leaked or smeared to close by grids of the true DOA, and hence the estimate of the source power vector  $\boldsymbol{\gamma}$  is  $K$ -peaksparse. The width of the peak around the true DOA will depend mainly on the SNR, the sample size  $L$  and the grid size  $M$ . Hence the CL-algorithms, CL-BCD and CL-CCD, will set the boolean variable `peak` as true in order to locate  $K$  significant peaks in  $\boldsymbol{\gamma}$ .

#### B. Simulation

Our simulation set-up is as follows. The array is ULA with half a wavelength interelement spacing and number of sensors is  $N = 20$ . The grid size is  $M = 1801$ , providing angular resolution  $\Delta\theta = 0.1^\circ$ . The number of MC trials is 1000. The SNR of  $k^{\text{th}}$  source is

$$\text{SNR}_k = \frac{\mathbb{E}[\|\mathbf{a}(\theta_k) s_{kl}\|^2]}{\mathbb{E}[\|\mathbf{e}_t\|^2]} = \frac{\sigma_k^2 \|\mathbf{a}(\theta_k)\|^2}{\sigma^2 N} = \frac{\sigma_k^2}{\sigma^2}$$

where  $\sigma_k^2 = \mathbb{E}[|s_{kl}|^2] = \gamma_{i_k}$  and we used that  $\|\mathbf{a}(\theta_k)\|^2 = N$ . The SNR is defined as average of source SNR-s, i.e.,  $\text{SNR (dB)} = \frac{10}{K} \sum_{k=1}^K \log_{10} \text{SNR}_k$ .

We compare the proposed CL-BCD, CL-CCD and CL-OMP against the Cramér-Rao lower bound and the following CL-based methods: **IAA**(-APES) [11, Table 2], **SAMV2** [12, Table I], and **SBL** variant of [16] (using  $b = 1$  in (20) in signal power update). We do not compare with M-SBL due to large number of atoms, making the method too computationally expensive in this scenario. For all methods (except for greedy CL-OMP which terminates after  $K$  iterations) we use (26) as the stopping criterion and set 500 as maximum number of iterations. As CL-CCD converges to the same fixed point as CL-BCD, we exclusively present the performance of the latter. Consequently, the legends and discussions in figures or in text only pertain to CL-BCD but are applicable to both methods. We also compare with conventional high-resolution methods: **MUSIC** [32] and **R-MUSIC** [33] (aka Root-MUSIC). We will seek the DOA peaks from MUSIC pseudospectrum using same DOA grid, and thus it has the same resolution as CL-based

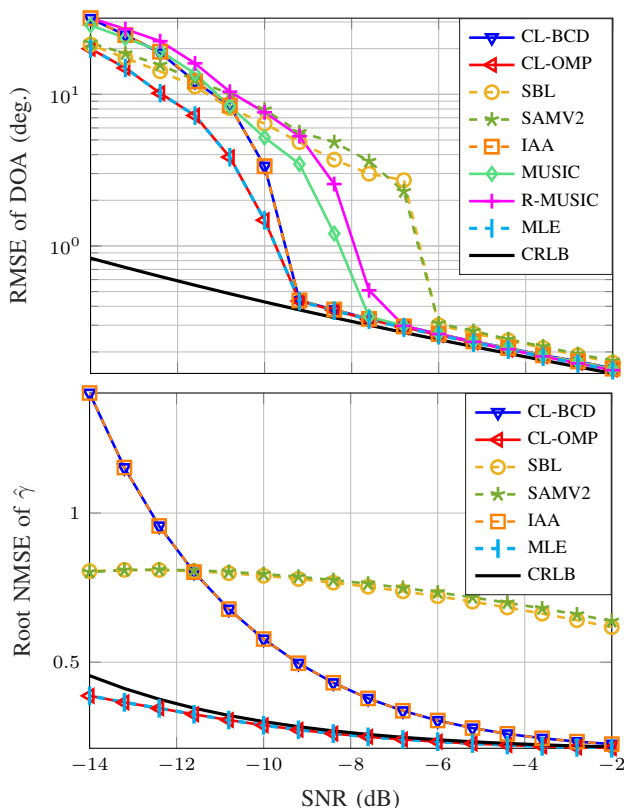


Fig. 4: RMSE of  $\hat{\theta}$  vs SNR (top panel) and root NMSE of  $\hat{\gamma}$  vs SNR (bottom panel) in a single source case with DOA  $\theta_1 = -25^\circ$ ;  $L = 25$ ,  $N = 20$ , and  $M = 1801$  ( $\Delta\theta = 0.1^\circ$ ).

algorithms. In the case of a single source, we also compare with the **MLE**, which can be obtained by solving

$$\hat{\theta}_{\text{ML}} = \arg \max_{\theta} \mathbf{a}(\theta)^H \hat{\Sigma} \mathbf{a}(\theta). \quad (37)$$

To find the maximizer in (37), we sweep through a dense grid of 18,001 points, yielding a resolution of  $0.01^\circ$ . It is worthwhile to note that SAMV2 uses the same signal power update as SBL. Thus we expect these two methods perform similarly in DOA estimation (i.e., identifying the support  $\mathcal{M}$ ), while possibly having some differences in actual estimates of signal powers. As discussed in subsection II-A, the signal power update of IAA is similar to FP update (18) and thus these two methods are expected to perform similarly in identifying the support  $\mathcal{M}$ .

In the first simulation setting, we have a single ( $K = 1$ ) source at  $\theta = -25^\circ$ . Figure 4 and Figure 5 display the performance of DOA and signal power estimation vs the SNR in terms of root MSE (RMSE) and root normalized MSE (NMSE), respectively, when  $L = 25$  and  $L = 200$ , respectively. Concerning DOA estimation, the following observations can be made: (a) The proposed CL-algorithms demonstrate the best performance; (b) CL-OMP performs comparably to the MLE across all SNR and snapshot ranges; (c) MUSIC and R-MUSIC exhibit essentially the same performance; (d) In the high SNR regime, CL-OMP, CL-BCD, IAA, MUSIC, and R-MUSIC perform similarly, attaining the CRLB; (e) SBL and SAMV2 exhibit similar performance, as anticipated, but

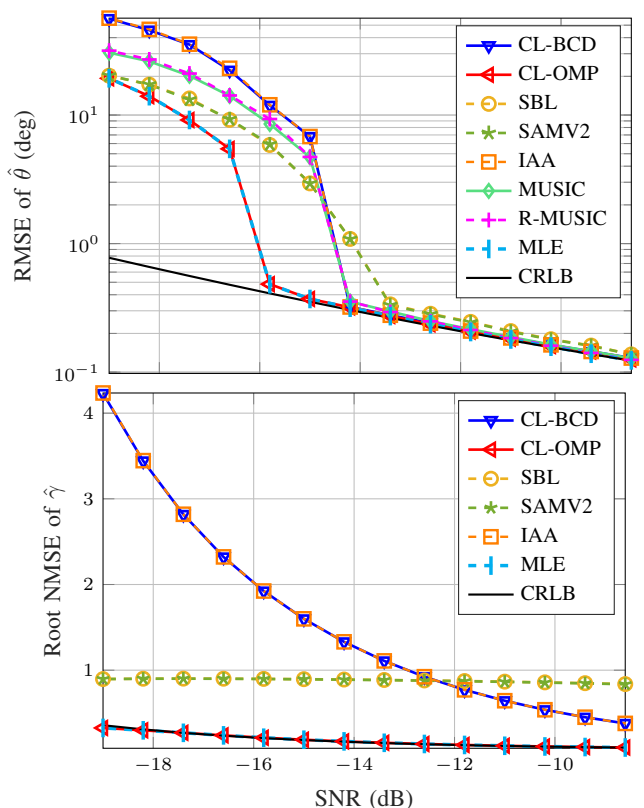


Fig. 5: RMSE of  $\hat{\theta}$  vs SNR (top panel) and root NMSE of  $\hat{\gamma}$  vs SNR (bottom panel) in a single source case with DOA  $\theta_1 = -25^\circ$ ;  $L = 200$ ,  $N = 20$ , and  $M = 1801$  ( $\Delta\theta = 0.1^\circ$ ).

they do achieve the same level of performance as the other methods. When  $L$  increases to 200, one can notice that CL-OMP and MLE improve their performance the most. The threshold where CL-OMP and MLE break down is  $< -15.8$  dB for  $L = 200$  while the 2nd best performing methods, CL-BCD and IAA, breakdown when SNR is  $< -14.2$  dB. SAMV2 and SBL show some improvement when the number of snapshots is larger. In terms of signal power estimation, CL-OMP and MLE exhibit impeccable performance, reaching the CRLB. On the other hand, CL-BCD and IAA provide accurate estimates of signal powers in the higher SNR regime, but their accuracy sharply deviates from the CRLB as SNR decreases. SAMV2 and SBL on the other hand provide clearly biased and inconsistent estimates of signal power estimates even in the high SNR regime.

Next, we investigate the impact of the true DOA, allowing the DOA of the source to range from  $-30^\circ$  to  $-80^\circ$  in 5 degree steps. The results are presented for a sample size of  $L = 25$  and SNR of  $-8$  dB in Figure 6. We can notice that CL-BCD and IAA start to deviate from the performance of CL-OMP more when the true DOA deviates significantly of array broadside. The performance of CL-OMP signal power estimate  $\hat{\gamma}$  is not affected by true DOA of the source. MUSIC and R-MUSIC exhibit erratic behaviour, and for some values of DOA, they encounter difficulties in identifying the true noise subspace due to the relatively small sample size. This issue results in a notably large value for the root NMSE.

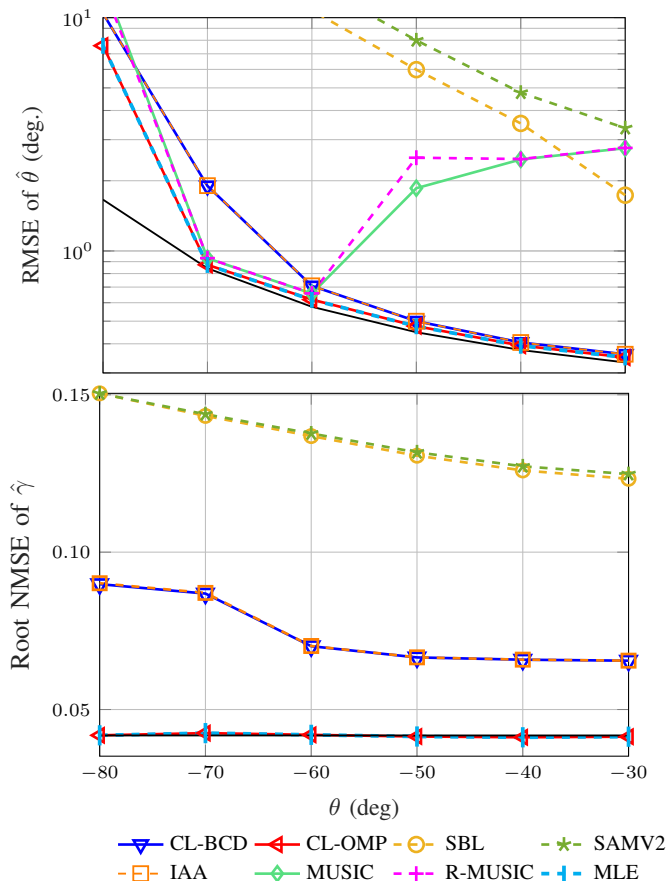


Fig. 6: RMSE of  $\hat{\theta}$  (top panel) and root NMSE of  $\hat{\gamma}$  (bottom panel) vs true DOA in single source case; SNR is  $-8$  dB,  $N = 20$ ,  $L = 25$ , and  $M = 1801$ . The black line displays the CRLB.

Next we consider the case of two source signals. The sources arrive from angles  $\theta_1 = -20.02^\circ$  and  $\theta_2 = 3.02^\circ$ , and are thus off the predefined grid. The 2nd source (closer to the array broadside) has 3dB higher power than the 1st source. We then calculate the DOA estimate  $\hat{\theta} = (\hat{\theta}_1, \hat{\theta}_2)^\top$  and the respective source power estimate  $\hat{\sigma}_s^2 = \hat{\gamma}_{\mathcal{M}}$  and their empirical RMSE  $\|\hat{\theta} - \theta\|$  and root NMSE  $\|\hat{\sigma}_s^2 - \sigma_s^2\|/\|\sigma_s^2\|$ , respectively, averaged over 1000 MC trials. The results for DOA estimation are displayed in Figure 7 when  $L = 25$  (bottom panel) and  $L = 125$  (top panel). As observed, the overall performance of the methods remains highly consistent with the single-source scenario. CL-OMP continues to exhibit the best performance across all SNR levels and various sample lengths. The second-best performing methods are CL-BCD and IAA, which demonstrate very similar performance. On the other hand, SBL and SAMV2 exhibit comparable but slightly less satisfactory performance compared to other competing methods. Top panel of Figure 8 displays the normalized RMSE of signal power estimates for snapshot size  $L = 25$ . The conclusions are equivalent with 1 source case: CL-OMP has impeccable performance for all SNR levels while IAA and CL-BCD provide consistent estimation only at high SNR regime, while SAMV2 and SBL estimates are heavily biased for all

SNR ranges.

Next we consider the effect of correlation of the source signals. Earlier studies have shown that the correlations of the source signals have little or no effect on support recovery performance of CL-based methods (see e.g., [34], [35]). Let the signal covariance  $\Sigma_s$  be of the form

$$\Sigma_s = \begin{pmatrix} \sigma_1^2 & \rho\sigma_1\sigma_2 \\ \rho\sigma_1\sigma_2 & \sigma_2^2 \end{pmatrix}$$

and we set correlation  $\rho$  as  $\rho = 0.95$ . Hence the signals have high correlation while their correlation phase is equal to 0. Otherwise the simulation set-up is as earlier. Figure 9 displays the DOA estimation performance vs the SNR when  $L = 25$  and  $L = 125$ , respectively. We can notice that the correlation did not bring essential differences between methods compared to uncorrelated case displayed in Figure 7. Thus all CL methods seem to be robust to correlation between the source signals. This is not the case for MUSIC and R-MUSIC which encounter complete failure. This is because their design is heavily dependent on the assumption of uncorrelated sources. The bottom panel of Figure 8 depicts the root NMSE of signal power estimate  $\hat{\sigma}_s^2$  in  $L = 25$  case. A comparison with the top panel plot ( $\rho = 0$ ) reveals that the curves are essentially equivalent. This further confirms the robustness of CL methods to source correlation, consistent with the findings of [34].

## VI. CONCLUSIONS

In this paper we revisited the covariance learning (CL) approach for SSR. First, relying on the Gaussian likelihood model and a known sensing matrix  $\mathbf{A}$ , we demonstrated that the MLE for the signal power  $\gamma$  satisfies the FP equation outlined in Lemma 1. Leveraging this property, we derived two cyclic algorithms for identifying the support of a sparse source signal matrix. The BCD and CCD algorithms update  $\gamma$  and  $\sigma^2$  either in blocks or coordinate-wise, using FP algorithm for computing the source powers. The main advantage of CL-CCD over CL-BCD can be in problems where noise power  $\sigma^2$  is known. In these cases, lines 6 to 8 in algorithm 2 can be skipped. Next we proposed a greedy pursuit CL algorithm, which we referred to CL-OMP due to its similarity with the (S)OMP algorithm. In the simulation study it was observed that CL-OMP outperforms its greedy-pursuit counterparts (SOMP or SNIHT) as well as M-SBL by a considerable margin when  $N$  is small, and the SNR is moderately low.

Subsequently, we evaluated the performance of the methods in SSR-based source localization, where the  $K$ -sparsity constraint is replaced with a  $K$ -peaksparsity constraint. We compared against state-of-the-art methods under a broad variate of settings and the Cramér-Rao lower bound was used as a benchmark. The proposed CL-algorithms outperformed competing methods especially in the low SNR regime, while they performed slightly better or similarly in high SNR. It was also observed that CL-OMP had better breakdown behaviour than other methods in low SNR. Additionally, the proposed CL algorithms demonstrated superior performance in accurately estimating the signal powers. Notably, CL-OMP stood out in

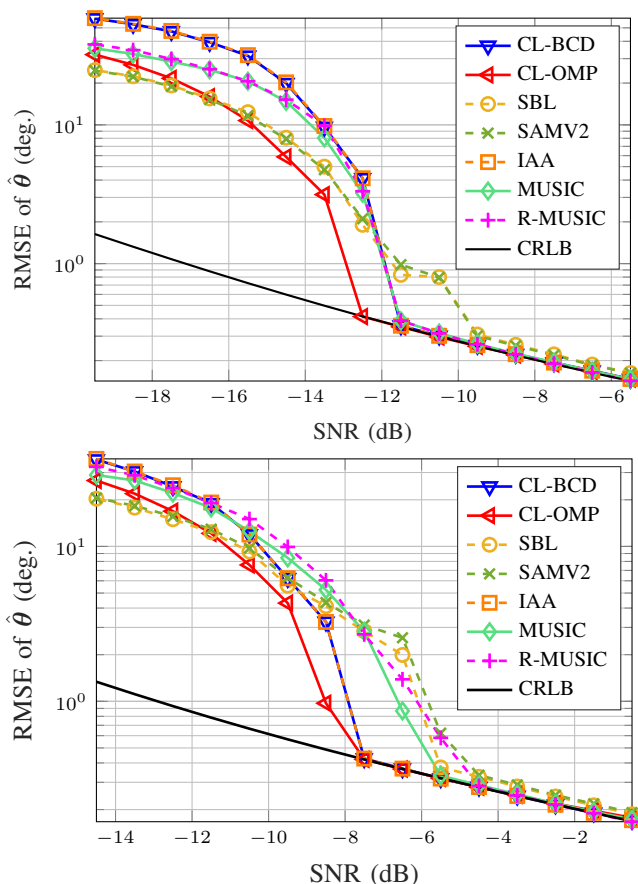


Fig. 7: RMSE of  $\hat{\theta}$  vs SNR in two sources case for  $L = 125$  (top panel) and  $L = 25$  (bottom panel);  $N = 20$ ,  $M = 1801$  ( $\Delta\theta = 0.1^\circ$ ),  $\theta_1 = -20.02^\circ$  and  $\theta_2 = 3.02^\circ$ , and the 2nd source has 3 dB higher power than the 1st source.

its own class, delivering nearly spot-on performance even in low SNR regimes.

There are many open questions to be addressed in future works. For example, (a) estimation of number of sources  $K$ ; (b) deriving performance guarantees (e.g., bounds on the probability of support recovery of CL-based methods); (c) addressing the non-Gaussian scenarios; (d) developing other greedy pursuit CL methods analogous to CoSaMP [36], gOMP [37], etc. Regarding items (b) and (c), works in [38] or [39] provide good starting points. Furthermore, there are several applications where the proposed CL-based sparse reconstructions could be useful. For example, they can be used as atom selection method in coupled dictionary learning algorithm [40] or activity detection method for massive machine type communications problems [13], [17], [41]. These explorations are left as future works.

## REFERENCES

- [1] M. F. Duarte and Y. C. Eldar, "Structured compressed sensing: From theory to applications," *IEEE Transactions on Signal Processing*, vol. 59, no. 9, pp. 4053–4085, 2011.
- [2] J. A. Tropp, A. C. Gilbert, and M. J. Strauss, "Algorithms for simultaneous sparse approximation. Part I: greedy pursuit," *Signal Processing*, vol. 86, pp. 572–588, 2006.

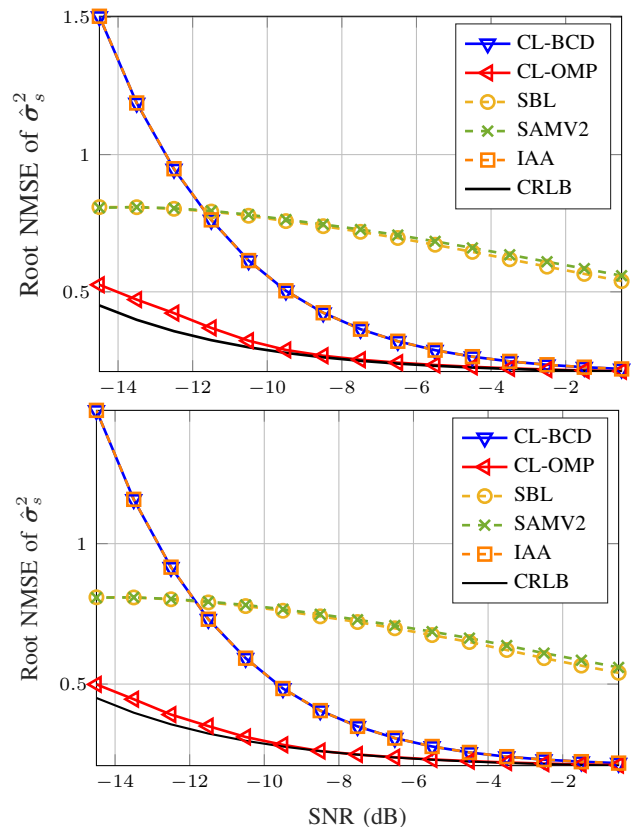


Fig. 8: Root NMSE of source signal power  $\hat{\sigma}_s^2$  vs SNR in two sources case for uncorrelated sources (top panel) and correlated sources (bottom panel) for  $\rho = 0.95$ ;  $L = 25$ ,  $N = 20$ ,  $M = 1801$  ( $\Delta\theta = 0.1^\circ$ ),  $\theta_1 = -20.02^\circ$ ,  $\theta_2 = 3.02^\circ$ , and the 2nd source has a 3 dB higher power.

- [3] J. A. Tropp, "Algorithms for simultaneous sparse approximation. Part II: convex relaxation," *Signal Processing*, vol. 86, pp. 589–602, 2006.
- [4] J. Chen and X. Huo, "Theoretical results on sparse representations of multiple-measurement vectors," *IEEE Transactions on Signal Processing*, vol. 54, no. 12, pp. 4634–4643, 2006.
- [5] Y. C. Eldar and H. Rauhut, "Average case analysis of multichannel sparse recovery using convex relaxation," *IEEE Transactions on Information Theory*, vol. 56, no. 1, pp. 505–519, 2010.
- [6] J. D. Blanchard, M. Cermak, D. Hanle, and Y. Jin, "Greedy algorithms for joint sparse recovery," *IEEE Transactions on Signal Processing*, vol. 62, no. 7, pp. 1694–1704, 2014.
- [7] M. E. Tipping, "Sparse bayesian learning and the relevance vector machine," *Journal of machine learning research*, vol. 1, no. Jun, pp. 211–244, 2001.
- [8] D. P. Wipf and B. D. Rao, "An empirical Bayesian strategy for solving the simultaneous sparse approximation problem," *IEEE Transactions on Signal Processing*, vol. 55, no. 7, pp. 3704–3716, 2007.
- [9] D. Wipf and S. Nagarajan, "Beamforming using the relevance vector machine," in *Proceedings of the 24th international conference on Machine learning*, 2007, pp. 1023–1030.
- [10] D. P. Wipf and B. D. Rao, "Sparse Bayesian learning for basis selection," *IEEE Transactions on Signal processing*, vol. 52, no. 8, pp. 2153–2164, 2004.
- [11] T. Yardibi, J. Li, P. Stoica, M. Xue, and A. B. Baggeroer, "Source localization and sensing: A nonparametric iterative adaptive approach based on weighted least squares," *IEEE Transactions on Aerospace and Electronic Systems*, vol. 46, no. 1, pp. 425–443, 2010.
- [12] H. Abeida, Q. Zhang, J. Li, and N. Merabtine, "Iterative sparse asymptotic minimum variance based approaches for array processing," *IEEE Transactions on Signal Processing*, vol. 61, pp. 933–944, 2012.
- [13] A. Fengler, S. Haghghatshoar, P. Jung, and G. Caire, "Non-Bayesian activity detection, large-scale fading coefficient estimation, and unsourced



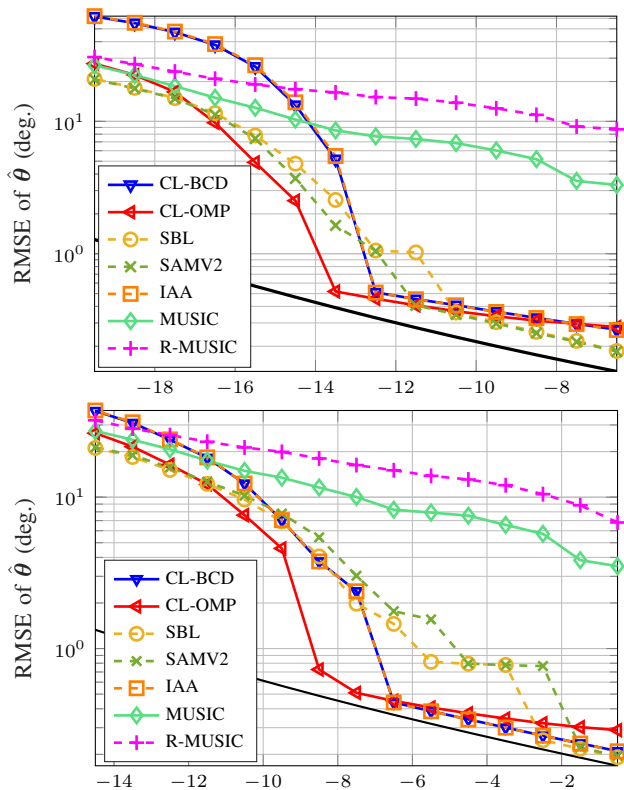


Fig. 9: RMSE of  $\hat{\theta}$  in the correlated 2 sources ( $\rho = 0.95$ ) case when  $L = 200$  (top panel) and  $L = 25$  (bottom panel);  $N = 20$ ,  $M = 1801$  ( $\Delta\theta = 0.1^\circ$ ),  $\theta_1 = -20.02^\circ$  and  $\theta_2 = 3.02^\circ$ , and the 2nd source has a 3dB higher power.

random access with a massive MIMO receiver,” *IEEE Transactions on Information Theory*, vol. 67, no. 5, pp. 2925–2951, 2021.

- [14] P. Stoica and R. Moses, *Introduction to Spectral Analysis*. Upper Saddle River, NJ: Prentice-Hall, 1997.
- [15] D. Malioutov, M. Cetin, and A. S. Willsky, “A sparse signal reconstruction perspective for source localization with sensor arrays,” *IEEE Transactions on Signal Processing*, vol. 53, no. 8, pp. 3010–3022, 2005.
- [16] S. Nannuru, K. L. Gemba, P. Gerstoft, W. S. Hodgkiss, and C. F. Mecklenbräuker, “Sparse bayesian learning with multiple dictionaries,” *Signal Processing*, vol. 159, pp. 159–170, 2019.
- [17] S. Haghghatshoar, P. Jung, and G. Caire, “Improved scaling law for activity detection in massive MIMO systems,” in *2018 IEEE International Symposium on Information Theory (ISIT)*. IEEE, 2018, pp. 381–385.
- [18] P. Stoica and A. Nehorai, “On the concentrated stochastic likelihood function in array signal processing,” *Circuits, Systems and Signal Processing*, vol. 14, no. 5, pp. 669–674, 1995.
- [19] Y. Bresler, “Maximum likelihood estimation of a linearly structured covariance with application to antenna array processing,” in *Fourth Annual ASSP Workshop on Spectrum Estimation and Modeling*. IEEE, 1988, pp. 172–175.
- [20] Z.-M. Liu, Z.-T. Huang, and Y.-Y. Zhou, “An efficient maximum likelihood method for direction-of-arrival estimation via sparse bayesian learning,” *IEEE Transactions on Wireless Communications*, vol. 11, no. 10, pp. 1–11, 2012.
- [21] P. Gerstoft, C. F. Mecklenbräuker, A. Xenaki, and S. Nannuru, “Multi-snapshot sparse Bayesian learning for DOA,” *IEEE Signal Processing Letters*, vol. 23, no. 10, pp. 1469–1473, 2016.
- [22] P. Stoica, P. Babu, and J. Li, “SPICE: A sparse covariance-based estimation method for array processing,” *IEEE Transactions on Signal Processing*, vol. 59, no. 2, pp. 629–638, 2010.
- [23] M. Elad, *Sparse and redundant representations*. New York: Springer, 2010.
- [24] G. Davis, S. Mallat, and M. Avellaneda, “Adaptive greedy approximations,” *Constructive approximation*, vol. 13, pp. 57–98, 1997.
- [25] H. Krim and M. Viberg, “Two decades of array signal processing: the parametric approach,” *IEEE Signal Processing Magazine*, vol. 13, no. 4, pp. 67–94, 1996.
- [26] H. L. Van Trees, *Detection, Estimation and Modulation theory, Part IV: Optimum array processing*. New York: Wiley, 2002, 1456 pages.
- [27] B. Ottersten, M. Viberg, P. Stoica, and A. Nehorai, “Exact and large sample maximum likelihood techniques for parameter estimation and detection in array processing,” in *Radar array processing*. Springer, 1993, pp. 99–151.
- [28] M. N. Tabassum and E. Ollila, “Sequential adaptive elastic net approach for single-snapshot source localization,” *The Journal of the Acoustical Society of America*, vol. 143, no. 6, pp. 3873–3882, 2018.
- [29] P. Gerstoft, A. Xenaki, and C. F. Mecklenbräuker, “Multiple and single snapshot compressive beamforming,” *The Journal of the Acoustical Society of America*, vol. 138, no. 4, pp. 2003–2014, 2015.
- [30] Z. Yang, J. Li, P. Stoica, and L. Xie, “Sparse methods for direction-of-arrival estimation,” in *Academic Press Library in Signal Processing, Volume 7*. Elsevier, 2018, pp. 509–581.
- [31] C. F. Mecklenbräuker, P. Gerstoft, and E. Ollila, “DOA M-estimation using sparse Bayesian learning,” in *IEEE International Conference on Acoustics, Speech and Signal Processing (ICASSP)*. IEEE, 2022, pp. 4933–4937.
- [32] R. O. Schmidt, “Multiple emitter location and signal parameter estimation,” *IEEE Transactions on Antennas and Propagation*, vol. 34, no. 3, pp. 276–280, 1986.
- [33] A. Barabell, “Improving the resolution performance of eigenstructure-based direction-finding algorithms,” in *IEEE International Conference on Acoustics, Speech, and Signal Processing (ICASSP)*, vol. 8. IEEE, 1983, pp. 336–339.
- [34] P. Stoica, P. Babu, and J. Li, “New method of sparse parameter estimation in separable models and its use for spectral analysis of irregularly sampled data,” *IEEE Transactions on Signal Processing*, vol. 59, no. 1, pp. 35–47, 2010.
- [35] R. R. Pote and B. D. Rao, “Robustness of sparse Bayesian learning in correlated environments,” in *IEEE International Conference on Acoustics, Speech and Signal Processing (ICASSP)*. IEEE, 2020, pp. 9100–9104.
- [36] D. Needell and J. A. Tropp, “CoSaMP: Iterative signal recovery from incomplete and inaccurate samples,” *Applied and Computational Harmonic Analysis*, vol. 26, no. 3, pp. 301–321, 2009.
- [37] J. Wang, S. Kwon, and B. Shim, “Generalized orthogonal matching pursuit,” *IEEE Transactions on Signal Processing*, vol. 60, no. 12, pp. 6202–6216, 2012.
- [38] G. Tang and A. Nehorai, “Performance analysis for sparse support recovery,” *IEEE Transactions on Information Theory*, vol. 56, no. 3, pp. 1383–1399, 2010.
- [39] C. F. Mecklenbräuker, P. Gerstoft, E. Ollila, and Y. Park, “Robust and sparse M-estimation of DOA,” *arXiv preprint arXiv:2301.06213*, 2023.
- [40] F. G. Veshki, N. Ouzir, S. A. Vorobyov, and E. Ollila, “Multimodal image fusion via coupled feature learning,” *Signal Processing*, vol. 200, p. 108637, 2022.
- [41] L. Liu, E. G. Larsson, W. Yu, P. Popovski, C. Stefanovic, and E. De Carvalho, “Sparse signal processing for grant-free massive connectivity: A future paradigm for random access protocols in the internet of things,” *IEEE Signal Processing Magazine*, vol. 35, no. 5, pp. 88–99, 2018.